A PRESSURIZED CYLINDRICAL SHELL WITH A FIXED END WHICH CONTAINS AN AXIAL PART-THROUGH OR THROUGH CRACK

by

O.S. Yahsi and F. Erdogan

December 1983

Lehigh University, Bethlehem, PA

THE NATIONAL AERONAUTICS AND SPACE ADMINISTRATION

GRANT NGR 39-007-011

A PRESSURIZED CYLINDRICAL SHELL WITH A FIXED END WHICH CONTAINS AN AXIAL PART-THROUGH OR THROUGH CRACK

by

O.S. Yahsi and F. Erdogan
Lehigh University, Bethlehem, PA

ABSTRACT

In this paper a cylindrical shell having a very stiff end plate or a flange is considered. It is assumed that near the end the cylinder contains an axial flaw which may be modeled as a part-through surface crack or a through crack. The primary objective is to study the effect of the end constraining on the stress intensity factor which is the main fracture mechanics parameter. The applied loads acting on the cylinder are assumed to be axisymmetric. Thus the crack problem under consideration is symmetric with respect to the plane of the crack and consequently only the Mode I stress intensity factors are nonzero. With this limitation, the general perturbation problem for a cylinder with a built-in end containing an axial crack is considered. Reissner's shell theory is used to formulate the problem. The part-through crack problem is treated by using a line-spring model. In the case of a crack tip terminating at the fixed end it is shown that the integral equations of the shell problem has the same generalized Cauchy kernel as the corresponding plane stress elasticity problem. Even though the problem is formulated for a general surface crack profile and arbitrary crack surface tractions, the numerical results are obtained only for a semi-elliptic part-through axial crack located at the inside or outside surface of the cylinder and for internal pressure acting on the cylinder. The stress intensity factors are calculated and presented for a relatively wide range of dimensionless length parameters of the problem.

1. Introduction

In recent past, solutions of crack problems in shells proved to be quite useful in studying fatigue and fracture of such important structural components as pipes, pressurized containers, and a great variety of other thin-walled structural elements (see, for example, [1] for applications to the fatigue crack propagation of part-through cracks and to the

estimation of net-ligament rupture loads in pipelines). The existing solutions which are based on either the classical shallow shell theory or a Reissner type transverse shear theory have all been given for "infinite" shells in the sense that the crack is assumed to be located sufficiently far away from the boundaries and all other sources of stress disturbance so that all interaction effects may be neglected. The differences between the asymptotic crack tip stress fields given by the classical theory and by a higher order theory have now been well-documented and will not be discussed in this paper (e.g., [2]), except to note that, particularly in the presence of local bending, the transverse shear theory appears to have clear advantages. The problems of a cylindrical shell with an axial crack, that with a circumferential crack and a spherical shell with a meridional crack have respectively been considered in [3], [4] and [5] by using Reissner's shell theory. The crack problem of toroidal shells with a positive or negative curvature ratio, including the effects of material orthotropy has been studied in [6]. The problem of an arbitrarily oriented crack in a cylindrical shell under general loading conditions is considered in [7]. The solutions given in [3]-[7] are all for a through crack.

The problem of surface cracks in shells is inherently a three-dimensional elasticity problem and appears to be analytically intractable. There are, however, some numerical solutions based on the technique of finite elements [8], [9], or boundary integral equations [10]. Recently, there has also been some applications of the line spring model developed in [11] for plates to surface crack problems in shells (see [12] for the results obtained by the transverse shear and [13] by the classical shell theory). Comparison of the results given in [12] with the finite element solution given in [9] shows that one could obtain surprisingly good results for the stress intensity factors along the border of a part-through crack in a shell by using the line spring model with a higher order shell theory and with reasonably accurate compliance functions for the corresponding plane strain edge crack problem under membrane and bending loads.

The primary objective of this paper is to study the influence of a stiffened end on the stress intensity factors in a pressurized cylindrical shell containing an axial through or a part-through crack near the end. Such problems may arise in pipes and cylindrical containers having flanges or end plates the bending and membrane stiffnesses of which are very high in comparison with those of the shell itself (e.g., heat exchanger tubing near the end plates). Thus, in formulating the problem it may be assumed that the end of the shell is "fixed", that is all components of the displacement and the rotation vectors are zero. The part-through crack problem is solved only for a semi-elliptic internal or external surface crack. However, the technique is quite general and can accommodate any crack profile within the confines of basic limitations of the line spring model. As in the corresponding plane elasticity problems, in the shell problem too the case of the crack tip touching the end stiffener requires special consideration with regard to the analysis of the crack tip singularity as well as to the method of solution.

2. The Basic Shell Equations

Referring to Appendix A for normalized and dimensionless quantities and to [3]-[5] for details of derivations, in terms of a stress function ϕ, displacement component w and the auxiliary functions ψ and Ω, the basic equilibrium equations of a cylindrical shell may be expressed as follows:

$$\nabla^4\phi - \left(\frac{\lambda_1}{\lambda}\right)^2 \frac{\partial^2 w}{\partial y^2} = 0 \quad , \tag{1}$$

$$\nabla^4 w + \lambda^2\lambda_1^2(1-\kappa\nabla^2) \frac{\partial^2\phi}{\partial y^2} = \lambda^4(1-\kappa\nabla^2) \frac{aq}{h} \quad , \tag{2}$$

$$\kappa\nabla^2\psi - \psi - w = 0 \quad , \tag{3}$$

$$\frac{\kappa(1-\nu)}{2} \nabla^2\Omega - \Omega = 0 \quad , \tag{4}$$

where $q(x,y)$ is the transverse shear loading and ψ and Ω are related to notations as follows [4]:

$$\beta_x = \frac{\partial \psi}{\partial x} + \frac{\kappa(1-\nu)}{2} \frac{\partial \Omega}{\partial y} \quad , \quad \beta_y = \frac{\partial \psi}{\partial y} - \frac{\kappa(1-\nu)}{2} \frac{\partial \Omega}{\partial x} \quad . \tag{5}$$

The shell and crack dimensions and the notation are described in Fig. 1. The normalized membrane, moment and transverse shear resultants are defined by

$$N_{xx} = \frac{\partial^2 \phi}{\partial y^2} \quad , \quad N_{yy} = \frac{\partial^2 \phi}{\partial x^2} \quad , \quad N_{xy} = - \frac{\partial^2 \phi}{\partial x \partial y} \quad , \tag{6}$$

$$M_{xx} = \frac{a}{h\lambda^4} \left(\frac{\partial \beta_x}{\partial x} + \nu \frac{\partial \beta_y}{\partial y} \right) \quad , \quad M_{yy} = \frac{a}{h\lambda^4} \left(\nu \frac{\partial \beta_x}{\partial x} + \frac{\partial \beta_y}{\partial y} \right) \quad ,$$

$$M_{xy} = \frac{a}{h\lambda^4} \frac{1-\nu}{2} \left(\frac{\partial \beta_x}{\partial y} + \frac{\partial \beta_y}{\partial x} \right) \quad , \tag{7}$$

$$V_x = \frac{\partial w}{\partial x} + \beta_x \quad , \quad V_y = \frac{\partial w}{\partial y} + \beta_y \quad . \tag{8}$$

To solve the problem, one may first consider a cylindrical shell without a crack which is fixed at $x_2 = 0$ plane and which is subjected to the given set of external loads. Since the problem is linear, the solution of the cracked shell problem may then be obtained by adding to this uncracked shell results a perturbation solution obtained from the cracked shell with a fixed end by using the equal and opposite of the stress and moment resultants from the first solution as the crack surface tractions. Thus, in the main crack problem one may assume that the transverse shear load q (such as pressure) is zero and the crack surface tractions are statically self-equilibrating.

3. Solution of the Differential Equations

By eliminating ϕ and by assuming that $q = 0$, from (1) and (2) we find

$$\nabla^4\nabla^4 w + \lambda_1^4(1-\kappa\nabla^2)\frac{\partial^2 w}{\partial y^2} = 0 \quad . \tag{9}$$

In the present study the primary interest is in the pressurized cylinder problem. Hence, in formulating the problem it will be assumed that the plane of the crack is a plane of symmetry with respect to loading as well as geometry. Therefore, for the shallow shell under consideration the solution of (9) may be expressed as

$$w(x,y) = \frac{1}{2\pi}\int_{-\infty}^{\infty} f_1(x,\alpha)e^{-i\alpha y}d\alpha + \frac{2}{\pi}\int_0^{\infty} f_2(y,\beta)\cos\beta x\, d\beta \quad . \tag{10}$$

Assuming the solution of the ordinary differential equations resulting from (10) and (9) of the form

$$f_1(x,\alpha) = R(\alpha,m)e^{mx} \quad , \quad f_2(y,\beta) = S(\beta,n)e^{ny} \quad , \tag{11}$$

the characteristic equations giving m and n may be obtained as follows:

$$m^8 - 4\alpha^2 m^6 + 6\alpha^4 m^4 - (4\alpha^2+\kappa\lambda_1^4)\alpha^4 m^2 + \alpha^4[\alpha^4+\lambda_1^4(1+\kappa\alpha^2)] = 0 \quad , \tag{12}$$

$$n^8 - (4\beta^2+\kappa\lambda_1^4)n^6 + (6\beta^4+\kappa\lambda_1^4\beta^2+\lambda_1^4)n^4 - 4\beta^6 n^2 + \beta^8 = 0 \quad . \tag{13}$$

Note that, ordered properly, the roots of (12) and (13) have the following property

$$\mathrm{Re}(m_j) < 0 \ , \ m_{j+4} = -m_j \ , \ j = 1,\ldots,4 \quad , \tag{14}$$

$$\mathrm{Re}(n_j) < 0 \ , \ n_{j+4} = -n_j \ , \ j = 1,\ldots,4 \quad . \tag{15}$$

If we now observe that for the particular shell under consideration (Fig. 1) $-\infty<y<0$, because of symmetry it is sufficient to consider the problem for $x>0$ only, and the external loads are local and are statically self-equilibrating (consequently all field quantities vanish as $x\to\infty$, $y\to-\infty$), by letting $R(\alpha,m_j)=R_j(\alpha)$ and $S(\beta,n_j)=S_j(\beta)$, the functions f_1 and

f_2 vanishing respectively at $x=\infty$ and $y=-\infty$ may be written as

$$f_1(x,\alpha) = \sum_{j=1}^{4} R_j(\alpha)e^{m_j x} \quad , \quad f_2(y,\beta) = \sum_{j=5}^{8} S_j(\beta)e^{n_j y} \quad , \tag{16}$$

where R_j, $(j=1,\ldots,4)$ and S_j, $(j=5,\ldots,8)$ are unknown functions.

Similarly, by expressing

$$\phi(x,y) = \frac{1}{2\pi}\int_{-\infty}^{\infty} g_1(x,\alpha)e^{-i\alpha y}d\alpha + \frac{2}{\pi}\int_{0}^{\infty} g_2(y,\beta)\cos\beta x \, d\beta \quad , \tag{17}$$

after obtaining w, from the coupled equations (1) and (2) the functions g_1 and g_2 may be obtained as

$$g_1(x,\alpha) = -\frac{\lambda_1^2\alpha^2}{\lambda^2}\sum_{1}^{4}\frac{R_j(\alpha)}{p_j^2}e^{m_j x} \quad , \; p_j=m_j^2-\alpha^2, \; (x>0) \quad , \tag{18}$$

$$g_2(y,\beta) = \frac{\lambda_1^2}{\lambda^2}\sum_{5}^{8}\frac{n_j^2 S_j(\beta)}{q_j^2}e^{n_j y} \quad , \; q_j=n_j^2-\beta^2, \; (y<0) \quad . \tag{19}$$

Expressing now Ω in the form

$$\Omega(x,y) = \frac{1}{2\pi}\int_{-\infty}^{\infty} h_1(x,\alpha)e^{-i\alpha y}d\alpha + \frac{2}{\pi}\int_{0}^{\infty} h_2(y,\beta)\sin\beta y \, d\beta \quad , \tag{20}$$

and assuming that

$$h_1(x,\alpha) = A(\alpha,r)e^{rx} \quad , \quad h_2(y,\beta) = B(\beta,s)e^{sy} \quad , \tag{21}$$

from (4) it can be shown that the functions h_1 and h_2 satisfying the conditions at $x=\infty$ and $y=-\infty$ may be expressed as

$$h_1(x,\alpha) = A_1(\alpha)e^{r_1 x} \quad , \; r_1 = -\left[\alpha^2 + \frac{2}{\kappa(1-\nu)}\right]^{\frac{1}{2}}, \; (0<x<\infty) \quad , \tag{22a,b}$$

$$h_2(y,\beta) = B_2(\beta)e^{s_2 y} \quad , \; s_2 = +\left[\beta^2 + \frac{2}{\kappa(1-\nu)}\right]^{\frac{1}{2}} \quad , \; (-\infty<y<0) \quad , \tag{23a,b}$$

where $A_1(\alpha) = A(\alpha, r_1)$ and $B_2(\beta) = B(\beta, s_2)$ are unknown functions.

Finally, one may easily show that the remaining differential equation (3) will also be satisfied and the solution will have the proper behavior at $x=\infty$, $y=-\infty$ if it is assumed that

$$\psi(x,y) = \frac{1}{2\pi}\int_{-\infty}^{\infty} \theta_1(x,\alpha)e^{-i\alpha y}d\alpha + \frac{2}{\pi}\int_{0}^{\infty} \theta_2(y,\beta)\cos\beta x\, d\beta \ , \tag{24}$$

$$\theta_1(x,\alpha) = \sum_{1}^{4} \frac{R_j(\alpha)}{\kappa p_j - 1} e^{m_j x} \ , \quad \theta_2(y,\beta) = \sum_{5}^{8} \frac{S_j(\beta)}{\kappa q_j - 1} e^{n_j y} \ , \tag{25}$$

where R_j, m_j, p_j, S_j, n_j and q_j are the same quantities which appear in (18) and (19).

The formulation given above for $x>0$, $y<0$ satisfies the conditions at infinity and contains ten unknown functions (R_j, S_j, A_1 and B_2). These functions are to be determined from the boundary conditions prescribed on $x=0$ and $y=0$.

4. The Boundary Conditions

Referring to Fig. 1 and assuming symmetry with respect to $x_1=0$ plane, the boundary conditions for a cylindrical shell fixed at $y=0$ and containing a through crack of length 2a along $x_1=0$, $-d<x_2<-b$ may be expressed as follows (see Appendix A for the normalized quantities)

$$u(x,0) = 0,\ v(x,0) = 0,\ w(x,0) = 0,\ \beta_x(x,0) = 0,\ \beta_y(x,0) = 0,\ (0<x<\infty) \ , \tag{26}$$

$$N_{xy}(0,y) = 0,\ M_{xy}(0,y) = 0,\ V_x(0,y) = 0,\ (-\infty<y<0) \ , \tag{27}$$

$$\left.\begin{aligned} &N_{xx}(+0,y) = F_1(y) \ , \ -d_1<y<-b_1 \ , \\ &u(0,y) = 0 \ , \ -\infty<y<-d_1,\ -b_1<y<0 \ , \end{aligned}\right\} \tag{28a,b}$$

$$\left.\begin{aligned} M_{xx}(+0,y) &= F_2(y) \ , \ -d_1<y<-b_1 \ , \\ \beta_x(0,y) &= 0 \ , \ -\infty<y<-d_1, \ -b_1<y<0 \end{aligned}\right\} \qquad (29a,b)$$

where $d_1 = d/a$, $b_1 = b/a$ and F_1 and F_2 are the crack surface tractions known from the uncracked shell solution. The displacement component w is given by (10) and (16) and the quantities β_x, β_y, N_{xy}, M_{xy}, V_x, N_{xx} and M_{xx} may easily be expressed in terms of the unknown functions R_j, S_j, A_1 and B_2 by substituting from the solution given in the previous section into (5)-(8). These expressions may be found in Appendix B. The displacements u and v are determined by using the Hooke's law and the strain displacement relations

$$\varepsilon_{ij} = \frac{1}{2}\left(u_{i,j}+u_{j,i}+Z_{,i}u_{3,j}+Z_{,j}u_{3,i}\right), \ (i,j = 1,2) \ , \qquad (30)$$

where $Z(x_1,x_2)$ gives the equation of the middle surface of the shell. Observing that $Z_{,22} = 0$, $Z_{,11} = -1/R$ and referring to Appendix A, it can be shown that

$$\frac{\partial^2 u}{\partial y^2} = 2(1+\nu)\frac{\partial N_{xy}}{\partial y} - \frac{\partial N_{yy}}{\partial x} + \nu\frac{\partial N_{xx}}{\partial x} + \frac{\lambda_1^2}{\lambda^2}\frac{\partial^2 w}{\partial y^2}x \ , \qquad (31)$$

$$\frac{\partial v}{\partial y} = N_{yy} - \nu N_{xx} \ , \qquad (32)$$

from which we obtain

$$u(x,y) = \frac{1}{2\pi}\frac{\lambda_1^2}{\lambda^2}\int_{-\infty}^{\infty}\sum_{1}^{4}\frac{(2+\nu)\alpha^2-m_j^2}{p_j^2}R_j(\alpha)m_j e^{m_j x - i\alpha y}\,d\alpha$$

$$+\frac{2}{\pi}\frac{\lambda_1^2}{\lambda^2}\int_{0}^{\infty}\sum_{5}^{8}\frac{(2+\nu)n_j^2}{q_j^2}S_j(\beta)\beta e^{n_j y}\sin\beta x\,d\beta + \frac{\lambda_1^2}{\lambda^2}xw(x,y) \ , \qquad (33)$$

$$v(x,y) = -\frac{i}{2\pi}\frac{\lambda_1^2}{\lambda^2}\int_{-\infty}^{\infty}\sum_{1}^{4}\frac{\nu\alpha^2+m_j^2}{p_j^2}R_j(\alpha)\alpha e^{m_j x - i\alpha y}\,d\alpha$$

$$-\frac{2}{\pi}\frac{\lambda_1^2}{\lambda^2}\int_{0}^{\infty}\sum_{5}^{8}\frac{n_j}{q_j^2}(\beta^2+\nu n_j^2)S_j(\beta)e^{n_j y}\cos\beta x\,d\beta,\quad (x>0,\ y<0). \qquad (34)$$

By substituting from (33), (34), (10), (16), (B.9) and (B.10) into (26) and by inverting the sine and cosine transforms we find

$$\sum_{5}^{8}\frac{(2+\nu)n_j^2-\beta^2}{q_j^2}S_j(\beta) = -\frac{1}{2\pi}\int_{-\infty}^{\infty}\sum_{1}^{4}\frac{(2+\nu)\alpha^2-m_j^2}{p_j^2(m_j^2+\beta^2)}R_j(\alpha)m_j\,d\alpha\,, \qquad (35)$$

$$\sum_{5}^{8}\frac{n_j(\beta^2+\nu n_j^2)}{q_j^2}S_j(\beta) = \frac{1}{2\pi}\int_{-\infty}^{\infty}\sum_{1}^{4}\frac{m_j^2+\nu\alpha^2}{p_j^2(m_j^2+\beta^2)}R_j(\alpha)\alpha m_j\,d\alpha\,, \qquad (36)$$

$$\sum_{5}^{8}S_j(\beta) = \frac{1}{2\pi}\int_{-\infty}^{\infty}\sum_{1}^{4}\frac{m_j R_j(\alpha)}{m_j^2+\beta^2}\,d\alpha\,, \qquad (37)$$

$$\sum_{5}^{8}\frac{\beta S_j(\beta)}{\kappa q_j-1} - \frac{\kappa(1-\nu)}{2}s_2B_2(\beta) = \frac{1}{2\pi}\int_{\infty}^{\infty}\sum_{1}^{4}\frac{\beta m_j R_j(\alpha)}{(\kappa p_j-1)(m_j^2+\beta^2)}\,d\alpha$$

$$-\frac{\kappa(1-\nu)i}{4\pi}\int_{-\infty}^{\infty}\frac{\alpha\beta A_1(\alpha)}{r_1^2+\beta^2}\,d\alpha\,, \qquad (38)$$

$$-\sum_{5}^{8}\frac{n_j S_j(\beta)}{\kappa q_j-1} + \frac{\kappa(1-\nu)}{2}\beta B_2(\beta) = \frac{i}{2\pi}\int_{-\infty}^{\infty}\sum_{1}^{4}\frac{\alpha m_j R_j(\alpha)}{(\kappa p_j-1)(m_j^2+\beta^2)}\,d\alpha$$

$$+\frac{\kappa(1-\nu)}{4\pi}\int_{-\infty}^{\infty}\frac{r_1^2A_1(\alpha)}{r_1^2+\beta^2}\,d\alpha\,. \qquad (39)$$

Consideration of the mixed boundary conditions (28) and (29) in mind, we now define the following new unknown functions:

$$G_1(y) = \frac{\partial}{\partial y} u(+0,y) \ , \ G_2(y) = \frac{\partial}{\partial y} \beta_x(+0,y) \ , \ (-\infty<y<0) \ . \tag{40}$$

From (33), (B.9) and (40) it can be shown that

$$G_1(y) = -\frac{i}{2\pi}\frac{\lambda_1^2}{\lambda^2}\int_{-\infty}^{\infty}\sum_1^4 \frac{(1+\nu)\alpha^2-p_j}{p_j^2} R_j(\alpha)\alpha e^{-i\alpha y}\, d\alpha \tag{41}$$

$$G_2(y) = -\frac{i}{2\pi}\int_{-\infty}^{\infty}\sum_1^4 \frac{m_j R_j(\alpha)}{\kappa p_j - 1}\alpha e^{-i\alpha y}\, d\alpha - \frac{\kappa(1-\nu)}{4\pi}\int_{-\infty}^{\infty}\alpha^2 A_1(\alpha)e^{-i\alpha y} d\alpha. \tag{42}$$

From (28), (29) and (40), if we observe that $G_1=0$, $G_2=0$ for $-\infty<y<-d_1$, $-b_1<y<0$, by defining

$$C_j(\alpha) = \int_{-d_1}^{-b_1} G_j(y)e^{i\alpha y}\, dy \ , \ (j = 1,2) \ , \tag{43}$$

and by using the expressions (B.3), (B.6) and (B.7) it can be shown that the homogeneous boundary conditions (27), (41) and (42) are equivalent to

$$\sum_1^4 \frac{m_j R_j(\alpha)}{p_j^2} = 0 \ , \tag{44}$$

$$\sum_1^4 \frac{m_j R_j(\alpha)}{\kappa p_j - 1} = i\left[\kappa(1-\nu)\alpha + \frac{1}{\alpha}\right] C_2(\alpha) \ , \tag{45}$$

$$\sum_1^4 m_j R_j(\alpha) = -\frac{i}{\alpha} C_2(\alpha) \ , \tag{46}$$

$$\sum_1^4 \frac{m_j R_j(\alpha)}{p_j} = -\frac{\lambda^2}{\lambda_1^2}\frac{i}{\alpha} C_1(\alpha) \ , \tag{47}$$

$$A_1(\alpha) = 2C_2(\alpha) \ . \tag{48}$$

From (44)-(47) one may easily solve for R_j and obtain expressions of the form

$$R_j(\alpha) = I[Q_j(\alpha)C_1(\alpha) + N_j(\alpha)C_2(\alpha)]$$

$$= \int_{-d_1}^{-b_1} \sum_{k=1}^{2} c_{jk}(\alpha,t)G_k(t)dt \ , \ (j=1,\ldots,4) \quad . \tag{49}$$

Substituting now from (48) and (49) into (35)-(39), the remaining unknowns may also be expressed as follows:

$$S_j(\beta) = \int_{-d_1}^{-b_1} \sum_{k=1}^{2} b_{jk}(\beta,t)G_k(t)dt \ , \ (j=1,\ldots,4) \ , \tag{50}$$

$$B_2(\beta) = \int_{-d_1}^{-b_1} \sum_{k=1}^{2} b_{5k}(\beta,t)G_k(t)dt \ , \tag{51}$$

where c_{jk} and b_{jk} are known functions. Thus, once G_1 and G_2 are determined (48)-(51) and Appendix B would give all the field quantities needed.

5. The Integral Equations

From the derivations given in the previous section it is seen that, in addition to the assumption $G_1=0=G_2$ for $-\infty<y<-d_1, -b<y<0$ used in (43) if G_1 and G_2 are also assumed to satisfy the conditions

$$\int_{-d_1}^{-b_1} G_j(y)dy = 0 \ , \ (j=1,2) \ , \tag{52}$$

Then all boundary conditions (26)-(29) except (28a) and (29a) would be satisfied. These two conditions may now be used to determine the unknown functions G_1 and G_2. Thus, by substituting from equations (B.1),

(B.4) and (48)-(51) into (28a) and (29a), we obtain

$$\lim_{x\to+0}\int_{-d_1}^{-b_1}\sum_{j=1}^{2}\left[\int_{-\infty}^{\infty}V_{kj}(x,\alpha)e^{i(t-y)\alpha}d\alpha+\int_{0}^{\infty}Y_{kj}(y,t,\beta)\cos x\beta d\beta\right]G_j(t)dt$$

$$=F_k(y),\ (k=1,2),\ (-d_1<y<-b_1) \tag{53}$$

where V_{kj} and Y_{kj} are very complicated but known functions. As $t\to y$ and for $b=0$ as $(t,y)\to 0$ the kernels in the integral equations (53) are expected to be unbounded. Since the singular behavior of the unknowns G_1 and G_2 will be dependent on the singular nature of the kernels, it is necessary to examine the asymptotic behavior of these kernels. In (53) the integrands of the inner integrals are bounded for all values of their arguments. Thus, any singularities the kernels may have must be due to the behavior of the integrands at $\alpha = \mp\infty$ and $\beta = \infty$, and these singularities may be separated by isolating the asymptotic parts of V_{kj} for $|\alpha|\to\infty$ and of Y_{kj} for $\beta\to\infty$. This can be done in closed form by first extracting the asymptotic values of $m_j(\alpha)$, $n_j(\beta)$, $r_1(\alpha)$ and $s_2(\beta)$ from the characteristic equations (12), (13), (22b) and (23b) and then by substituting these values into the expressions of V_{kj} and Y_{kj}. From the characteristic equations it can be shown that for large values of $|\alpha|$ and β we have

$$m_j(\alpha)=-|\alpha|\left(1+\frac{p_j}{2\alpha^2}-\frac{p_j^2}{8\alpha^4}+\ldots\right),\ (j=1,\ldots,4)\ , \tag{54}$$

$$n_j(\beta)=\beta\left(1+\frac{q_j}{2\beta^2}-\frac{q_j^2}{8\beta^4}+\ldots\right),\ (j=5,\ldots,8)\ , \tag{55}$$

$$r_1(\alpha)=-|\alpha|\left(1+\frac{1}{\kappa(1-\nu)\alpha^2}-\ldots\right)\ , \tag{56}$$

$$s_2(\beta)=\beta\left(1+\frac{1}{\kappa(1-\nu)\beta^2}-\ldots\right)\ . \tag{57}$$

By using (54)-(57) and by adding and subtracting the asymptotic values of V_{kj} and Y_{kj} in (53), after evaluating the singular terms of the kernels in closed form, the integral equations (53) may finally be expressed as follows:

$$\int_{-d_1}^{-b_1}\left[\frac{1}{t-y}+\frac{\nu^2+6\nu-3}{(\nu+1)(3-\nu)}\frac{1}{t+y}-\frac{6(1+\nu)}{3-\nu}\frac{y}{(t+y)^2}+\frac{4(1+\nu)}{3-\nu}\frac{y^2}{(t+y)^3}\right]G_1(t)dt$$
$$+\int_{-d_1}^{-b_1}k_{11}(y,t)G_1(t)dt+\int_{-d_1}^{-b_1}k_{12}(y,t)G_2(t)dt=2\pi F_1(y)\ ,$$
$$-d_1<y<-b_1\ , \qquad (58)$$

$$(1-\nu^2)\int_{-d_1}^{-b_1}\left[\frac{1}{t-y}+\frac{\nu^2+6\nu-3}{(\nu+1)(3-\nu)}\frac{1}{t+y}-\frac{6(1+\nu)}{3-\nu}\frac{y}{(t+y)^2}+\frac{4(1+\nu)}{3-\nu}\frac{y^2}{(t+y)^3}\right]G_2(t)dt$$
$$+\int_{-d_1}^{-b_1}k_{21}(y,t)G_1(t)dt+\int_{-d_1}^{-b_1}k_{22}(y,t)G_2(t)dt=2\pi\lambda^4\frac{h}{a}F_2(y)\ ,$$
$$-d_1<y<-b_1\ , \qquad (59)$$

where the kernels k_{ij}, $(i,j=1,2)$ are known bounded functions. It should be noted that the integral equations (58) and (59) must be solved under conditions (52).

For $b_1>0$ the integral equations (58) and (59) have simple Cauchy-type kernels and have a solution of the form [14]

$$G_k(y)=H_k(y)/[-(y+d_1)(y+b_1)]^{\frac{1}{2}}\ ,\ -d_1<y<-b_1,\ (k=1,2) \qquad (60)$$

where H_1 and H_2 are unknown bounded functions. In this case the integral equations may be solved numerically by using the technique described,

for example, in [15]. On the other hand for $b_1 = 0$ (that is, if the crack tip $y = -b_1$ is extended to the fixed end), it is seen that the kernels have singular terms in addition to $(t-y)^{-1}$ which become unbounded as $t\to 0$ and $y\to 0$ together. The singular parts of the kernels shown separately in (58) and (59) are typically the generalized Cauchy kernels. Because of these kernels the solution no longer has the square-root singularity given by (60). From (58) and (59) we first observe that the dominant kernels in the two equations are identical. Consequently, the singular behavior of G_1 and G_2 (or u and β_x) at the crack tips would be identical. This, of course, is the physically expected result. Next, to obtain the singular behavior of the solution we express G_1 and G_2 as

$$G_k(y) = P_k(y)/[-y^{\gamma}(y+d_1)^{\omega}] \ , \ 0<\mathrm{Re}(\gamma,\omega)<1, \ (k=1,2), \ (-d_1<y<0), \qquad (61)$$

where the functions P_1 and P_2 are bounded and unknown and the unknown constants γ and ω are determined by substituting from (61) into (58) and (59) and by using the function-theoretic method (see, for example, [15]). Thus, from (58), (59) and (61) the characteristic equations giving γ and ω may be obtained as follows:

$$\cos\pi\gamma + \frac{\nu^2+6\nu-3}{(\nu+1)(3-\nu)} + \frac{2(1+\nu)}{3-\nu}\ \gamma\ (\gamma+2) = 0 \ , \qquad (62)$$

$$\cot\pi\omega = 0 \ . \qquad (63)$$

The acceptable root of (63) is 1/2 which is the expected power of singularity for the crack tip $y=-d_1$ embedded in a homogeneous medium. It may be shown that (62) is identical to the plane stress version of the characteristic equation for the corresponding plane elasticity problem [16]. For example, for $\nu=0.3$ it is found that $\gamma = 0.24165$ is the acceptable root. In this special case too the system of integral equations (58) and (59) may again be solved numerically by following the technique described in [15].

6. Stress Intensity Factors

After solving the integral equations the asymptotic behavior of the stress state around the crack tips may be examined by using the expressions given in Appendix B. For the embedded crack (i.e., for b>0) the problem is the same as in an infinite shell which has been discussed previously in detail elsewhere (see, [3]-[6]). For the crack tip at the fixed end b=0 the asymptotic behavior of the stress state would be identical to the plane stress problem considered in [16] and only the related stress intensity factor needs to be given. One should note that as shown in [3]-[6], unlike the asymptotic results obtained from the classical theory, the membrane and bending resultants given by the Reissner's theory have identical behavior around the crack tips and this behavior is in turn identical to that given by the plane elasticity theory. Thus, to describe the stress state around the crack tips all one needs to do is to determine a set of thickness-dependent stress intensity factors.

The in-plane components of the stress state in the shell are given by

$$\sigma_{ij}(x_1,x_2,x_3) = \sigma^m_{ij} + \sigma^b_{ij},\ \sigma^m_{ij}(x_1,x_2) = \frac{N_{ij}(x_1,x_2)}{h},$$

$$\sigma^b_{ij}(x_1,x_2,x_3) = \frac{12x_3}{h^3} M_{ij}(x_1,x_2),\ (i,j=1,2), \tag{64}$$

where superscripts m and b refer to membrane and bending stresses. In the symmetric problem under consideration only the Mode I stress state exists around the crack tips. For the embedded crack the corresponding stress intensity factors at the crack tips $x_2 = -d$ and $x_2 = -b$ (Fig. 1) may, therefore, be defined as follows:

$$k_1(-b,x_3) = \lim_{x_2\to -b} \sqrt{2(x_2+b)}\ \sigma_{11}(0,x_2,x_3),$$

$$k_1(-d,x_3) = \lim_{x_2\to -d} \sqrt{-2(x_2+d)}\ \sigma_{11}(0,x_2,x_3)\ . \tag{65a,b}$$

These stress intensity factors may be calculated from the asymptotic analysis of the stresses around the crack tips. However, they may also be calculated directly from the integral equations (58) and (59) without lengthy asymptotic analysis. To do this we first observe that the left hand sides of (58) and (59) give the expressions for N_{xx} and M_{xx} on x=0 outside as well as inside the crack $(-d_1<y<-b_1)$, and only the dominant kernels contribute to the stress singularity. Thus referring to (64) and (65), after some calculations it may easily be shown that

$$k_1(-b,x_3) = -\frac{E}{2}\sqrt{a}\,[H_1(-b_1) + \frac{x_3}{a} H_2\,(-b_1)]\ ,$$

$$k_1(-d,x_3) = \frac{E}{2}\sqrt{a}\,[H_1(-d_1) + \frac{x_3}{a} H_2(-d_1)]\ , \qquad (66a,b)$$

where H_1 and H_2 are related to G_1 and G_2 through (60) and are the main calculated results.

For b = 0 the angular distribution of stresses and the stress intensity factors will depend on the dominant parts of the integral equations (58) and (59). Since the dominant kernels obtained for the shell problem are identical to the plane elasticity problem, (aside from the magnitude of the stress intensity factors) the analysis and the results would also be the same. The details of the asymptotic analysis may be found in [16]. In this problem it is particularly important to note that the stress intensity factor k_1 is a measure of the amplitude of all in-plane stresses σ_{ij}, (i,j=1,2) around the crack tip y=0, there is no "cleavage" stress σ_{11} in the "second medium" (which is rigid) in terms of which k_1 may be defined, stress state around the crack tip may be calculated in terms of k_1 and the angular distributions given in [16], and k_1 may easily be defined in terms of the crack surface displacement $(au+x_3\beta_x)$. Similar to [16], from the dominant part of the integral equations the stress intensity factor at the crack tip $x_2=-b=0$ may be obtained as

$$k_1(0,x_3) = -\frac{4E[2-\nu-\gamma(1-\nu)]}{(1+\nu)(3-\nu)\sin\pi\gamma}\left[P_1(0) + \frac{x_3}{a}P_2(0)\right] \tag{67}$$

After the determination of the thickness-dependent stress intensity factor k_1 the stress state near the crack tip $x_2=0$ may be obtained from

$$\sigma_{ij}(r,\theta,x_3) \cong \frac{k_1(0,x_3)}{\sqrt{2}\,r^{\gamma}} f_{ij}(\theta) \quad , \tag{68}$$

where (r,θ) are the polar coordinates in (x_1,x_2) plane and the functions f_{ij} may be found in [16](*). In this case at the embedded crack tip $x_2=-d$ the relation between the stress intensity factor and the crack surface displacement leading to (66b), namely

$$k_1(-d,x_3) = \frac{E}{2}\lim_{x_2\to -d}\sqrt{2(x_2+d)}\,\frac{\partial}{\partial x_2}\left[u_1(+0,x_2) + x_3\beta_{11}(+0,x_2)\right] \tag{69}$$

is still valid and, therefore, referring to (61) k_1 may be calculated from

$$k_1(-d,x_3) = \frac{E}{2^{\gamma+\frac{1}{2}}}\sqrt{a}\left[P_1(-d_1) + \frac{x_3}{a}P_2(-d_1)\right] \quad . \tag{70}$$

7. The Part-Through Crack Problem

In this paper the part-through crack problem described in Fig. 1 will be treated by using the line-spring model. The particular version of the model used with the Reissner's plate or shell theory is discussed in [17] and [12] in detail. Since for the problem under consideration the method to be followed and the compliance coefficients to be used in the line spring model would be identical to those given in [17] and [12], only the results and no analytical details will be discussed in this paper.

(*) The distributions given for the greatest stiffness ratio in [16] may be used as an approximation to the rigid end problem.

In the symmetrically loaded shell having a symmetrically oriented crack shown in Fig. 1, it is clear that only the Mode I stress intensity factor would be nonzero along the crack front. At a location y along the crack front this stress intensity factor is calculated from [12]

$$k_1(y) = \sqrt{h}\,[\sigma(y)g_t(\xi) + m(y)g_b(\xi)]\ ,\ \xi = L/h\ . \tag{71}$$

The functions σ and m are defined by

$$\sigma(y) = \frac{N(x_2)}{h} = \frac{N(ay)}{h}\ ,\ m(y) = \frac{6M(x_2)}{h^2} = \frac{6M(ay)}{h^2}\ , \tag{72}$$

where N and M are the membrane and bending resultants which replace the net ligament under the surface crack and L is the crack depth (Fig. 1). The functions g_t and g_b are essentially the shape factors for the plane strain problem of a strip of thickness h which contains an edge crack of depth L and is subjected to uniform tension or cylindrical bending. These shape factors are given by

$$g_t(\xi) = \sqrt{\xi}\ (1.1216 + 6.5200\xi^2 - 12.3877\xi^4 + 89.0554\xi^6 - 188.6080\xi^8 + 207.3870\xi^{10} - 32.0524\xi^{12})\ ,$$

$$g_b(\xi) = \sqrt{\xi}\ (1.1202 - 1.8872\xi + 18.0143\xi^2 - 87.3851\xi^3 + 241.9124\xi^4 - 319.9402\xi^5 + 168.0105\xi^6)\ . \tag{73a,b}$$

To determine σ and m the integral equations (58) and (59) are modified to incorporate the effect of the net ligament. This is done by replacing F_1 and F_2 (which are equal and opposite to N_{xx} and M_{xx} calculated from the uncracked shell solution) as follows:

$$F_1(y) \to F_1(y) + \frac{\sigma(y)}{E}\ ,\ F_2(y) \to F_2(y) + \frac{m(y)}{6E}\ . \tag{74}$$

By using also the linear dependence between the pairs (σ,m) and (u,β_x) [12], the integral equations are then modified as

$$-\gamma_{tt}(y)\int_{-d_1}^{y} G_1(t)dt \mp \gamma_{tb}(y)\int_{-d_1}^{y} G_2(t)dt + \frac{1}{2\pi}\int_{-d_1}^{-b_1} k_s(y,t)G_1(t)dt$$

$$+ \frac{1}{2\pi}\int_{-d_1}^{-b_1} \sum_{1}^{2} k_{1j}(y,t)G_j(t)dt = F_1(y),\ -d_1<y<-b_1\ , \qquad (75)$$

$$\mp\gamma_{bt}(y)\int_{-d_1}^{y} G_1(t)dt - \gamma_{bb}(y)\int_{-d_1}^{y} G_2(t)dt + \frac{a(1-\nu^2)}{2\pi h\lambda^4}\int_{-d_1}^{-b_1} k_s(y,t)G_2(t)dt$$

$$\frac{a}{2\pi h\lambda^4}\int_{-d_1}^{-b_1} \sum_{1}^{2} k_{2j}(y,t)G_j(t)dt = F_2(y),\ -d_1<y<-b_1\ , \qquad (76)$$

where k_s is the generalized Cauchy kernel given in (58) and (59), the upper (i.e., -) the lower (i.e., +) signs are to be used for the outer and the inner surface crack, respectively.

After solving (75) and (76) for G_1 and G_2, u and β_x, and then σ and m are evaluated as follows:

$$u(+0,y) = \int_{-d_1}^{y} G_1(t)dt\ ,\ \beta_x(+0,y) = \int_{-d_1}^{y} G_2(t)dt\ , \qquad (77)$$

$$\sigma(y) = E[\gamma_{tt}u \pm \gamma_{tb}\beta_x],\ m(y) = 6E[\gamma_{bt}u \pm \gamma_{bb}\beta_x]\ , \qquad (78)$$

where the + and - signs are to be used for the outer and the inner crack, respectively. The functions $\gamma_{ij}(y)$, $(i,j=t,b)$ are known in terms of g_t and g_b (see [12] or [17]) .

8. The Results for a Pressurized Cylinder

As an example we consider a cylinder which is fixed in one end and is internally pressurized (Fig. 1). The cylinder is assumed to be sufficiently long so that the perturbation field of the crack interacts with one end only. The crack problem is solved by using the equal and opposite of the stress resultants N_{11} and M_{11} obtained in Appendix C from the uncracked shell solution as the crack surface tractions in the integral equations (58) and (59) or (75) and (76). In the through crack problem, as seen from (66), the stress intensity factors are linearly dependent on the thickness coordinate x_3. Thus, one may distinguish a "membrane" and a "bending" component of the stress intensity factor. We could therefore define the following normalized stress intensity factors:

$$k_m(\alpha_i) = \frac{k_1(\alpha_i,0)}{(p_oR_i/h)\sqrt{a}}, \quad k_b(\alpha_i) = \frac{k_1(\alpha_i,h/2)-k_1(\alpha_i,0)}{(p_oR_i/h)\sqrt{a}}, \qquad (79a,b)$$

where $\alpha_1 = -b$, $\alpha_2 = -d$ identify the crack tip, k_1 is defined by (65) and is calculated from (66), p_o is the internal pressure, 2a is the crack length, and R_i is the inner radius and h the thickness of the cylinder. The normalizing stress intensity factor $(p_oR_i/h)\sqrt{a}$ corresponds to the value in a flat plate under a uniform membrane stress (p_oR_i/h) and having the same size crack as the shell.

Tables 1 and 2 show the calculated results obtained for certain values of the dimensionless length parameters R/h, a/h and c/a of the problem, where c defines the crack location. The tables clearly show the influence of the end stiffener in reducing the stress intensity factors. As c increases the stress intensity factors at both ends approach the infinite cylinder values. The effect of the end stiffener and the curvature on the stress intensity factors can be seen somewhat better in Fig. 2 where some limited information is displayed. The figure shows the membrane component of the normalized stress intensity factor defined by (79a) as a function of the crack location c for a

fixed crack length a=3h and for various curvature ratios R/h. It is important again to observe that as c→a, or as the crack tip approaches the end stiffener, generally the stress intensity factors decrease and, furthermore, k_m at x_2=-b tends to zero. This may easily be explained by noting that for c=a there is a change in the nature of stress singularity, i.e.,

$$\sigma_{ij} \tilde{=} \frac{k_1(-b)}{\sqrt{2r}} \quad \text{for } c>a \quad \text{or} \quad b>0 \quad , \tag{80}$$

$$\sigma_{ij} \tilde{=} \frac{k_1(0)}{\sqrt{2}\, r^{\gamma}} = \frac{k_1(0) r^{\frac{1}{2}-\gamma}}{\sqrt{2r}} \quad \text{for } c=a \text{ or } b=0 \quad , \tag{81}$$

where r is a small distance from the crack tip and $k_1(-b)$ and $k_1(0)$ are finite constants. Thus, from (80) and (81) it is seen that the stress intensity factor based on the definition of the conventional square root singularity becomes

$$\lim_{b\to 0} k_1(-b) \tilde{=} \lim_{\substack{r\to 0 \\ b\to 0}} \sqrt{2r}\, \sigma_{ij} = \lim_{r\to 0} k_1(0) r^{\frac{1}{2}-\gamma} = 0 \quad . \tag{82}$$

A second somewhat curious observation one may make from Fig. 2 is that for smaller values of R/h there seems to be a slight "overshoot" in the stress intensity factor $k_m(-d)$ before it tends to the infinite cylinder value. The explanation for this may be found in the uncracked cylinder solution which indicates that in the perturbation region the end stiffener may cause a slight bulging of the cylinder in radial direction.

In Tables 1 and 2 the column c/a = 1 corresponds to the crack terminating at the end stiffener, (i.e., b=0). In this case the stress intensity factor k_1 at x_2=0 is calculated from (67). Despite relatively large magnitudes of these stress intensity factors, as indicated above, since the stress singularity at this point is a weaker singularity

(i.e., $\gamma \leq \frac{1}{2}$, see (68)), there is actually a reduction in the amplitude of the stress field as $b \to 0$.

The results obtained from the part-through crack solution are given in Tables 3-10. In all these calculations it is assumed that the crack has a semi-elliptic profile as shown in Fig. 1 for which the crack depth is given by

$$L(x_2) = L_o\sqrt{1-(x_2+c)^2/a^2} \ , \ (-d<x_2<-b) \tag{83}$$

or

$$L(y) = L_o\sqrt{1-(y+c_1)^2} \ , \ y = x_2/a, \ c_1 = c/a, \ (-c_1-1<y<-c_1+1): \tag{84}$$

The stress intensity factors shown in the Tables are calculated from (71) and are normalized as follows:

$$k_t(\bar{x}) = \frac{k_1(x_2)}{k_{ot}} \ , \ k_{ot} = \frac{p_o R_i}{h}\sqrt{h}\, g_t(\xi_o) \ , \ \xi_o = \frac{L_o}{h} \ , \tag{85}$$

$$k_b(\bar{x}) = \frac{k_1(x_2)}{k_{ob}} \ , \ k_{ob} = \frac{p_o R_i}{h}\sqrt{h}\, g_b(\xi_o) \ , \ \xi_o = \frac{L_o}{h} \ , \tag{86}$$

where $\bar{x} = y+c_1 = (x_2+c)/a$ and k_t is the contribution of the membrane component N_{11} and k_b that of the bending component M_{11} of the external loading (see, equations (C9) and (C10)). The total Mode I stress intensity factor along the crack front is then given by

$$k_1(\bar{x}) = k_t(\bar{x}) + k_b(\bar{x}) \ , \ (-1<\bar{x}<1) \ . \tag{87}$$

The normalizing stress intensity factors k_{ot} and k_{ob} are the corresponding edge crack values obtained from the plane strain solution of an edge-notched strip under a membrane stress $N_\infty = p_o R_i/h$ or a bending moment $M_\infty = p_o R_i h/6$. The expressions of g_t and g_b are given by (73). For values of L_o/h which are used in the numerical calculations they are also given by

$L_o/h = \xi_o$	0.2	0.4	0.6	0.8
$\sqrt{h/L_o}\, g_t(\xi_o)$	1.3674	2.1119	4.035	11.988
$\sqrt{h/L_o}\, g_b(\xi_o)$	1.0554	1.2610	1.915	4.691

In the tables contributions of the membrane and bending loads are shown separately in order to give some idea about the nature of the loading. The results show that even though generally the membrane component is the dominant stress intensity factor, near the fixed end, particularly for relatively small cracks the stress intensity factor resulting from the bending component of the external load may be the more significant one.

Tables 3-7 show the normalized stress intensity factors k_t and k_b at the maximum penetration point ($\bar{x} = y+c_1 = (x_2+c)/a = 0$) of a semielliptic inner or outer surface crack in the pressurized cylinder for various combinations of the dimensionless length parameters L_o/h, a/h, c/a and R/h. In all calculations given in this paper it is assumed that the Poisson's ratio ν is 0.3. The effect of ν on the stress intensity factors, however, is known to be rather insignificant [4].

Tables 8-10 show some examples for the distribution of the normalized stress intensity factors k_t and k_b along the crack front. As expected, for cracks very near the end the stress intensity distribution is highly nonsymmetric (with respect to the mid-point $\bar{x} = (x_2+c)/a = 0$) and as c increases it becomes more symmetric (see, for example, Table 9, $c/a = 10$).

Some sample results showing the variation of the total stress intensity factor are given in Figures 3 and 4. The total stress intensity factor k_1 is calculated from (85)-(87) as follows:

$$k_1(x_2) = k_{ot}k_t(\bar{x}) + k_{ob}k_b(\bar{x})$$
$$= \left(\frac{p_o R_i}{h}\sqrt{L_o}\right)\left[k_t(\bar{x})\sqrt{h/L_o}\, g_t(L_o/h) + k_b(\bar{x})\sqrt{h/L_o}\, g_b(L_o/h)\right] . \quad (88)$$

Figure 3 shows the stress intensity factor at the deepest penetration point of the crack (i.e., for $L=L_o$ at $x_2=-c$) as a function of the distance c to the end of the cylinder for a fixed crack size ($a/h = 1$, $L_o/h = 0.4$) and for various values of the curvature. This figure too shows the drastic reduction in the stress intensity factor caused by the end stiffener and by the increase in the cylinder radius. The results shown in Fig. 3 are obtained for an outer crack. For greater values of R/h if the crack is very near the cylinder end then the stress intensity factor may be negligibly small or may even be negative. This shows the importance of the bending moment M_{11} which develops in the cylinder as a result of constraining the end. Needless to say, when k_1 becomes negative along any portion of the crack front the problem is no longer a simple crack problem and must be treated as a crack-contact problem. In such a case the solution given in this paper is, of course, not valid. The crack contact problem is highly nonlinear in which the additional unknown function L(y) has to be determined by using the information that the contact is "smooth" and consequently the total stress intensity factor along that portion of the crack front is zero. Even though the problem can be solved by a complicated iterative scheme, quite clearly it has no practical value. From a viewpoint of structural failure, the important problems in practice are those of crack opening not crack closing.

Finally, some examples showing the distribution of the total stress intensity factor k_1 along the crack front are shown in Fig. 4. Curves a and b show k_1 respectively for an outer and an inner crack for the same cylinder and crack dimensions ($R/h = 10$, $L_o/h = 0.4$, $a/h = 1$, $c/a = 1.1$). The difference between the two results is again primarily due to bending moment M_{11} caused by the end constraints. Curve c shows the distribution of k_1 for a longer internal crack ($a/h = 3$, $c/a = 1.1$, $R/h = 10$, $L_o/h = 0.4$). The intensification in k_1 along the crack front away from the fixed end observed in curve c may be due to slight cylinder bulging as well as to the decrease in the influence of the end constraints. Curve d shows k_1 for an outer crack away from the end ($c/a = 10$, $a/h = 1$, $R/h = 10$, $L_o/h = 0.4$) for which the distribution as expected is nearly symmetric.

Acknowledgements

This work was partially supported by the National Science Foundation under the Grant MEA-8209083, and by NASA-Langley under the Grant NGR 39-007-011. It was completed by the second author during his stay at the Fraunhofer-Institut für Weikstoffmechanik in Freiburg, Germany as an Alexander von Humboldt senior U.S. Scientist Awardee.

9. References

1. F. Erdogan and H. Ezzat, "Elastic Plastic Fracture of Cylindrical Shells Containing a Part-Through Circumferential Crack", J. Pressure Vessel Technology, Trans. ASME, Vol. 104, pp. 609-614, 1983.

2. J.K. Knowles and N.M. Wang, "On Bending of an Elastic Plate Containing a Crack", J. Math. and Phys., Vol. 39, pp. 223-236 (1960).

3. S. Krenk, "Influence of Transverse Shear on an Axial Crack in a Cylindrical Shell", Int. Journal of Fracture, Vol. 14, pp. 123-143 (1978).

4. F. Delale and F. Erdogan, "Transverse Shear Effect in a Circumferentially Cracked Cylindrical Shell", Quarterly of Applied Mathematics, Vol. 37, pp. 239-258 (1979).

5. F. Delale and F. Erdogan, "Effect of Transverse Shear and Material Orthotropy in a Cracked Spherical Cap", Int. J. Solids Structures, Vol. 15, pp. 907-926 (1979).

6. F. Delale and F. Erdogan, "The Crack Problem in a Specially Orthotropic Shell with Double Curvature", Engineering Fracture Mechanics, Vol. 18, pp. 529-544, 1983.

7. O.S. Yahsi and F. Erdogan, "A Cylindrical Shell with an Arbitrary Oriented Crack", Int. J. Solids Structures, Vol. 20 (1984) (to appear).

8. J.C. Newman and I.S. Raju, "Stress Intensity Factors for Internal Surface Cracks in Cylindrical Pressure Vessels", NASA Technical Memorandum 80073 (July 1979).

9. J.J. McGowan and M. Raymond, "Stress Intensity Factor Solutions for Internal Longitudinal Semi-Elliptic Surface Flaws in a Cylinder under Arbitrary Loadings", ASTM-STP 677, Fracture Mechanics (1979).

10. J. Heliot, R.C. Labbens and A. Pellisier-Tanou, "Semi-Elliptic Cracks in a Cylinder Subjected to Stress Gradients", ASTM-STP 677, Fracture Mechanics (1979).

11. J.R. Rice and N. Levy, "The Part-Through Surface Crack in an Elastic Plate", J. Appl. Mech., Vol. 39, Trans. ASME, pp. 185-194 (1972).

12. F. Delale and F. Erdogan, "Application of the Line Spring Model to a Cylindrical Shell Containing a Circumferential or Axial Part-Through Crack", J. Appl. Mech., Vol. 39, Trans. ASME, pp. 97-102 (1982).

13. D.M. Parks, "The Inelastic Line-Spring: Estimates of Elastic Plastic Fracture Mechanics Parameters for Surface-Cracked Plates and Shells", Paper 80-C2/PVP-109, ASME (1980).

14. N.I. Muskhelishvili, Singular Integral Equations, Noordhoff, Groningen, The Netherlands (1953).

15. F. Erdogan, "Mixed Boundary Value Problems in Mechanics", Mechanics Today, S. Nemat-Nasser, ed., Vol. 4, Pergamon Press, pp. 1-86 (1978).

16. T.S. Cook and F. Erdogan, "Stresses in Bonded Materials with a Crack Perpendicular to the Interface", Int. J. Engng. Sci., Vol. 10, pp. 677-697 (1972).

17. F. Delale and F. Erdogan, "Line-Spring Model for Surface Cracks in a Reissner Plate", Int. J. Engng. Sci., Vol. 19, pp. 1331-1340 (1981).

18. S. Timoshenko and S. Woinowsky-Krieger, Theory of Plates and Shells, McGraw-Hill, New York (1959).

APPENDIX A

Dimensionless and normalized quantities

$$x = x_1/a,\ y = x_2/a,\ z = x_3/a,\ b_1 = \frac{b}{a},\ c_1 = \frac{c}{a},\ d_1 = \frac{d}{a}\ , \tag{A.1}$$

$$u = u_1/a,\ v = u_2/a,\ w = u_3/a\ , \tag{A.2}$$

$$\beta_x = \beta_1,\ \beta_y = \beta_2,\ \phi(x,y) = \frac{F(x_1,x_2)}{a^2Eh}\ , \tag{A.3}$$

$$\sigma_{xx} = \sigma_{11}/E,\ \sigma_{yy} = \sigma_{22}/E,\ \sigma_{xy} = \frac{\sigma_{12}}{E},\ \sigma_{xz} = \frac{\sigma_{13}}{B},\ \sigma_{yz} = \frac{\sigma_{23}}{B}\ , \tag{A.4}$$

$$N_{xx} = \frac{N_{11}}{hE},\ N_{yy} = \frac{N_{22}}{hE},\ N_{xy} = \frac{N_{12}}{hE},\ \sigma_{ij} = \frac{N_{ij}}{h},\ (i=1,2)\ , \tag{A.5}$$

$$M_{xx} = M_{11}/h^2E,\ M_{yy} = M_{22}/h^2E,\ M_{xy} = M_{12}/h^2E\ , \tag{A.6}$$

$$V_x = V_1/hB,\ V_y = V_2/hB,\ B = \frac{5E}{12(1+\nu)}\ , \tag{A.7}$$

$$\lambda_1^4 = 12(1-\nu^2)a^4/h^2R^2,\ \lambda^4 = 12(1-\nu^2)a^2/h^2,\ \kappa = E/B\lambda^4\ . \tag{A.8}$$

For dimensions and notation see Figure 1.

APPENDIX B

Expressions for stress resultants and rotations.

$$N_{xx}(x,y) = \int_{-\infty}^{\infty} \sum_{1}^{4} \alpha^4 T_{1j} d\alpha + \int_{0}^{\infty} \sum_{5}^{8} n_j^2 L_{1j} \cos\beta x \, d\beta \, , \tag{B.1}$$

$$N_{yy}(x,y) = -\int_{-\infty}^{\infty} \sum_{1}^{4} \alpha^2 m_j^2 T_{1j} d\alpha - \int_{0}^{\infty} \sum_{5}^{8} L_{1j} \beta^2 \cos\beta x \, d\beta, \tag{B.2}$$

$$N_{xy}(x,y) = -i\int_{-\infty}^{\infty} \sum_{1}^{4} \alpha^3 m_j T_{1j} d\alpha + \int_{0}^{\infty} \sum_{5}^{8} \beta n_j L_{1j} \sin\beta x \, d\beta, \tag{B.3}$$

$$M_{xx}(x,y) = \int_{-\infty}^{\infty} \sum_{1}^{4} (m_j^2 - \nu\alpha^2) T_{2j} d\alpha - \int_{0}^{\infty} \sum_{5}^{8} (\beta^2 - \nu n_j^2) L_{2j} \cos\beta x \, d\beta$$

$$- \frac{(1-\nu)ia}{h\lambda^4} \int_{-\infty}^{\infty} \alpha r_1 T_3 d\alpha + \frac{(1-\nu)a}{h\lambda^4} \int_{0}^{\infty} \beta s_1 L_3 \cos\beta x \, d\beta \, , \tag{B.4}$$

$$M_{yy}(x,y) = \int_{-\infty}^{\infty} \sum_{1}^{4} (\nu m_j^2 - \alpha^2) T_{2j} d\alpha - \int_{0}^{\infty} \sum_{5}^{8} (\nu\beta^2 - n_j^2) L_{2j} \cos\beta x \, d\beta$$

$$+ \frac{(1-\nu)ia}{h\lambda^4} \int_{-\infty}^{\infty} \alpha r_1 T_3 d\alpha - \frac{(1-\nu)a}{h\lambda^4} \int_{0}^{\infty} s_1 \beta \cos\beta x \, d\beta \, , \tag{B.5}$$

$$M_{xy}(x,y) = -i(1-\nu)\int_{-\infty}^{\infty} \sum_{1}^{4} \alpha m_j T_{2j} d\alpha - (1-\nu)\int_{0}^{\infty} \sum_{5}^{8} \beta n_j L_{2j} \sin\beta x \, d\beta$$

$$- \frac{(1-\nu)a}{2h\lambda^4} \int_{-\infty}^{\infty} (\alpha^2 + r_1^2) T_3 d\alpha + \frac{(1-\nu)a}{2h\lambda^4} \int_{0}^{\infty} (s_1^2 + \beta^2) L_3 \sin\beta x \, d\beta, \tag{B.6}$$

$$V_x(x,y) = \frac{\kappa h\lambda^4}{a} \int_{-\infty}^{\infty} \sum_{1}^{4} p_j m_j T_{2j} d\alpha - \frac{\kappa h\lambda^4}{a} \int_{0}^{\infty} \sum_{5}^{8} \beta q_j L_{2j} \sin\beta x \, d\beta$$

$$-i \int_{-\infty}^{\infty} \alpha T_3 d\alpha + \int_{0}^{\infty} s_1 L_3 \sin\beta x \, d\beta \, , \tag{B.7}$$

$$V_y(x,y) = -\frac{i\kappa h\lambda^4}{a}\int_{-\infty}^{\infty}\sum_{1}^{4}\alpha p_j T_{2j}\,d\alpha + \frac{\kappa h\lambda^4}{a}\int_{0}^{\infty}\sum_{5}^{8} q_j n_j L_{2j}\cos\beta x\,d\beta$$

$$-\int_{-\infty}^{\infty} r_1 T_3\,d\alpha - \int_{0}^{\infty}\beta L_3\cos\beta x\,d\beta \quad , \tag{B.8}$$

$$\beta_x(x,y) = \frac{h\lambda^4}{a}\int_{-\infty}^{\infty}\sum_{1}^{4} m_j T_{2j}\,d\alpha - \frac{h\lambda^4}{a}\int_{0}^{\infty}\sum_{5}^{8}\beta L_{2j}\sin\beta x\,d\beta$$

$$-i\int_{-\infty}^{\infty}\alpha T_3\,d\alpha + \int_{0}^{\infty} s_1\sin\beta x\,d\beta \quad , \tag{B.9}$$

$$\beta_y(x,y) = -\frac{ih\lambda^4}{a}\int_{-\infty}^{\infty}\sum_{1}^{4}\alpha T_{2j}\,d\alpha + \frac{h\lambda^4}{a}\int_{0}^{\infty}\sum_{5}^{8} n_j L_{2j}\cos\beta x\,d\beta$$

$$-\int_{-\infty}^{\infty} r_1 T_3\,d\alpha - \int_{0}^{\infty}\beta\, B_2\cos\beta x\,d\beta \quad . \tag{B.10}$$

where

$$T_{1j}(x,y,\alpha) = \frac{1}{2\pi}\frac{\lambda_1^2}{\lambda^2}\frac{R_j(\alpha)}{p_j^2}e^{m_j x - i\alpha y} \quad ,$$

$$T_{2j}(x,y,\alpha) = \frac{1}{2\pi}\frac{a}{h\lambda^4}\frac{R_j(\alpha)}{\kappa p_j - 1}e^{m_j x - i\alpha y} \quad ,$$

$$T_3(x,y,\alpha) = \frac{\kappa(1-\nu)}{4\pi}A_1(\alpha)e^{r_1 x - i\alpha y} \quad ,$$

$$L_{1j}(y,\beta) = \frac{2}{\pi}\frac{\lambda_1^2}{\lambda^2}\frac{n_j^2}{q_j^2}S_j(\beta)e^{n_j y} \quad ,$$

$$L_{2j}(y,\beta) = \frac{2}{\pi}\frac{a}{h\lambda^4}\frac{1}{\kappa q_j - 1}S_j(\beta)e^{n_j y} \quad ,$$

$$L_3(y,\beta) = \frac{\kappa(1-\nu)}{\pi}B_2(\beta)e^{s_2 y} \quad .$$

APPENDIX C

Stresses in the uncracked pressurized shell with a fixed end

In this simple axisymmetric case by assuming that the ends of the cylinder is closed and by observing that

$$u_1 = 0,\ \beta_1 = 0,\ \varepsilon_{11} = u_3/R,\ N_{22} = pR/2 \quad , \tag{C.1}$$

following the notation of [18] we can write

$$N_{22} = \frac{Eh}{1-\nu^2}\left(\frac{du_2}{dx_2} - \nu\,\frac{u_3}{R}\right) \quad , \quad N_{11} = \frac{Eh}{1-\nu^2}\left(-\frac{u_3}{R} + \nu\,\frac{du_2}{dx_2}\right) \quad , \tag{C2a,b}$$

$$M_{22} = -D\,\frac{d^2u_3}{dx_2^2} \quad , \quad M_{11} = \nu M_{22},\ D = \frac{Eh^3}{12(1-\nu^2)} \quad , \tag{C3a-c}$$

$$\frac{d^2M_{22}}{dx_2^2} + \frac{1}{R}\,N_{11} = p \tag{C.4}$$

where p is the internal pressure and x_2 is the only independent variable. From (C.1)-(C.4) it may be shown that

$$N_{11} = -\frac{Eh}{R}\,u_3 + \frac{\nu pR}{2} \quad , \tag{C.5}$$

$$\frac{d^4u_3}{dx_2^4} + 4\beta^4 u_3 = -\frac{2-\nu}{2}\,\frac{p}{D} \quad , \quad (-\infty<x_2<0),\ \beta^4 = \frac{Eh}{4R^2D} \quad . \tag{C.6}$$

Solution of (C.6) which is bounded at $x_2=-\infty$ and satisfies

$$u_3(0) = 0 \quad , \quad \frac{d}{dx_2}\,u_3(0) = 0 \tag{C.7}$$

becomes

$$u_3(x_2) = \frac{2-\nu}{2}\frac{pR^2}{Eh}\left[e^{\beta x_2}(\cos\beta x_2 - \sin\beta x_2) - 1\right] , \quad (x_2<0). \tag{C.8}$$

From (C.8), (C.5) and (C.3) it then follows that

$$N_{11}(x_2) = -\frac{2-\nu}{2} e^{\beta x_2}(\cos\beta x_2 - \sin\beta x_2) + pR , \tag{C.9}$$

$$M_{11}(x_2) = \frac{\nu(2-\nu)}{4\beta^2} p\, e^{\beta x_2}(\cos\beta x_2 + \sin\beta x_2) , \quad (-\infty<x_2<0) \quad . \tag{C.10}$$

Table 1. Membrane component of the normalized stress intensity factor k_m in a pressurized cylinder with a fixed end containing an axial through crack, ν=0.3.

R/h	c/a \ a/h	k_m(-b)					k_m(-d)				
		1	1.1	1.5	2	10	1	1.1	1.5	2	10
5	1	2.933	0.151	0.346	0.572	1.286	0.535	0.575	0.734	0.915	1.284
	2	5.754	0.284	0.839	1.340	1.645	1.082	1.158	1.425	1.613	1.645
	3	9.164	0.490	1.500	2.015	2.067	1.583	1.687	1.985	2.081	2.067
	10	43.555	2.853	4.703	4.912	4.923	4.422	4.605	4.850	4.929	4.953
10	1	2.128	0.119	0.235	0.364	1.168	0.355	0.380	0.483	0.611	1.158
	2	3.728	0.181	0.477	0.814	1.331	0.713	0.765	0.967	1.167	1.332
	3	5.658	0.277	0.840	1.338	1.589	1.067	1.142	1.402	1.573	1.588
	10	25.183	1.627	3.467	3.605	3.620	3.139	3.314	3.551	3.602	3.620
25	1	1.622	0.102	0.172	0.236	1.063	0.232	0.247	0.303	0.373	1.081
	2	2.423	0.128	0.275	0.448	1.147	0.431	0.463	0.590	0.743	1.142
	3	3.397	0.165	0.424	0.728	1.259	0.650	0.697	0.882	1.074	1.260
	10	13.151	0.860	2.218	2.480	2.469	2.031	2.160	2.429	2.466	2.469
100	1	1.345	0.093	0.140	0.167	0.685	0.159	0.166	0.188	0.215	0.744
	2	1.598	0.100	0.169	0.232	1.045	0.229	0.242	0.296	0.367	1.063
	3	1.956	0.111	0.213	0.325	1.107	0.321	0.343	0.434	0.548	1.097
	10	5.563	0.269	0.839	1.336	1.542	1.049	1.126	1.380	1.536	1.542
200	1	1.293	0.092	0.134	0.154	0.496	0.146	0.150	0.165	0.182	0.546
	2	1.431	0.095	0.150	0.190	0.885	0.184	0.193	0.227	0.272	0.937
	3	1.633	0.101	0.173	0.241	1.058	0.238	0.253	0.311	0.388	1.070
	10	3.864	0.184	0.507	0.874	1.308	0.745	0.801	1.007	1.199	1.308

able 2. Bending component of the normalized stress intensity factor k_b in a pressurized cylinder with a fixed end containing an axial through crack, $\nu = 0.3$.

/h		k_b(-b)					k_b(-d)				
	c/a / a/h	1	1.1	1.5	2	10	1	1.1	1.5	2	10
	1	-20.927	-0.312	-0.085	0.030	0.115	0.051	0.061	0.100	0.136	0.115
	2	-14.250	-0.183	0.069	0.220	0.185	0.151	0.160	0.196	0.211	0.185
	3	-11.925	-0.196	0.178	0.266	0.188	0.180	0.189	0.220	0.220	0.189
	10	-6.839	-0.284	-0.582	-0.869	-0.935	-0.491	-0.593	-0.808	-0.920	-0.933
0	1	-23.006	-0.316	-0.134	-0.051	0.080	-0.014	-0.007	0.029	0.069	0.076
	2	-13.258	-0.170	-0.019	0.116	0.147	0.095	0.103	0.138	0.167	0.146
	3	-9.371	-0.167	0.077	0.223	0.183	0.143	0.153	0.191	0.208	0.183
	10	-5.995	-0.221	0.025	-0.144	-0.199	-0.029	-0.046	-0.111	-0.181	-0.199
5	1	-25.930	-0.326	-0.180	-0.130	0.086	-0.092	-0.086	-0.057	-0.021	0.073
	2	-12.693	-0.165	-0.091	0.000	0.090	0.023	0.029	0.063	0.098	0.090
	3	-8.235	-0.144	-0.027	0.098	0.138	0.079	0.087	0.123	0.154	0.137
	10	-4.065	-0.194	0.256	0.210	0.148	0.159	0.172	0.199	0.174	0.148
00	1	-28.812	-0.339	-0.227	-0.210	0.069	-0.179	-0.178	-0.164	-0.142	0.077
	2	-12.677	-0.171	-0.160	-0.118	0.081	-0.082	-0.079	-0.052	-0.022	0.070
	3	-7.162	-0.140	-0.116	-0.052	0.071	-0.023	-0.018	0.020	0.048	0.066
	10	-1.933	-0.134	0.104	0.243	0.197	0.134	0.147	0.234	0.235	0.198
00	1	-29.841	-0.342	-0.242	-0.236	0.019	-0.209	-0.209	-0.202	-0.187	0.036
	2	-12.761	-0.175	-0.184	-0.160	0.081	-0.127	-0.125	-0.108	-0.082	0.082
	3	-6.911	-0.144	-0.148	-0.106	0.077	-0.073	-0.070	-0.047	-0.013	0.066
	10	-1.418	-0.115	0.018	0.153	0.163	0.091	0.101	0.145	0.180	0.163

Table 3. Normalized stress intensity factors in a cylindrical shell with a fixed end containing an axial semielliptic surface crack and subjected to internal pressure, R/h = 5.

Outer Crack, R/h = 5, ν = 0.3

a/h	c/a	L_o = 0.2h		L_o = 0.4h		L_o = 0.6h		L_o = 0.8h	
		$k_t(0)$	$k_b(0)$	$k_t(0)$	$k_b(0)$	$k_t(0)$	$k_b(0)$	$k_t(0)$	$k_b(0)$
1	1	.304	-.0679	.185	-.0367	.0895	-.0108	.0273	.0009
	1.1	.331	-.0490	.202	-.0276	.0984	-.0087	.0300	.0003
	1.5	.446	.0160	.277	.0064	.137	.0009	.0417	-.0008
	2	.585	.0639	.368	.0338	.183	.0099	.0559	-.0009
	10	.918	-.0018	.588	-.0011	.295	-.0004	.0898	.000
2	1	.629	.0671	.444	.0382	.246	.0132	.0818	.0000
	1.1	.680	.0778	.484	.0459	.270	.0168	.0905	.0007
	1.5	.856	.0895	.621	.0580	.355	.0248	.121	.0030
	2	.979	.0641	.718	.0441	.415	.0206	.143	.0033
	10	.993	.000	.737	.000	.430	.000	.147	.000
3	1	.880	.0906	.673	.0605	.410	.0273	.150	.0041
	1.1	.926	.0859	.713	.0590	.439	.0279	.162	.0048
	1.5	1.040	.0489	.812	.0373	.511	.0206	.193	.0051
	2	1.050	.0107	.835	.0099	.532	.0067	.202	.0022
	10	1.020	.000	.817	.000	.523	.000	.148	.000
10	1	1.060	-.0020	.935	-.0014	.705	-.0005	.338	.0002
	1.1	1.060	-.0009	.935	-.0008	.707	-.0004	.339	.000
	1.5	1.060	.0001	.941	.000	.714	.000	.344	.000
	2	1.070	.000	.944	.000	.720	.000	.348	.000
	10	1.070	.000	.952	.000	.732	.000	.357	.000

Inner Crack, R/h = 5, ν = 0.3

1	1	.299	.0670	.177	.0351	.0849	.0099	.0265	-.0010
	1.1	.325	.0482	.193	.0263	.0928	.0080	.0290	-.0005
	1.5	.437	-.0157	.262	-.0059	.127	-.0006	.0399	.0008
	2	.572	-.0625	.346	-.0311	.168	-.0082	.0529	.0014
	10	.898	.0018	.551	.0010	.270	.0003	.0844	.000
2	1	.612	-.0651	.410	-.417	.216	-.0097	.0728	.0011
	1.1	.662	-.0756	.445	-.0411	.236	-.0128	.0797	.0006
	1.5	.833	-.0869	.567	-.0517	.305	-.0190	.104	-.0009
	2	.952	-.0621	.656	-.0392	.355	-.0157	.121	-.0015
	10	.968	.000	.676	.000	.370	.000	.126	.000
3	1	.857	-.0876	.613	-.0532	.347	-.0202	.123	-.0013
	1.1	.902	-.0832	.649	-.0521	.369	-.0208	.132	-.0020
	1.5	1.010	-.0475	.739	-.0331	.427	-.0156	.154	-.0028
	2	1.030	-.0105	.762	-.0088	.445	-.0052	.161	-.0014
	10	1.000	.000	.750	.000	.442	.000	.160	.000
10	1	1.050	-.0018	.896	.0008	.628	-.0003	.269	-.0005
	1.1	1.050	.0009	.898	.0005	.632	.000	.272	-.0002
	1.5	1.060	.000	.906	.000	.644	.000	.281	.000
	2	1.060	.000	.911	.000	.652	.000	.286	.000
	10	1.060	.000	.920	.000	.665	.000	.294	.000

Table 4. Normalized stress intensity factors in a cylindrical shell with a fixed end containing an axial semielliptic surface crack and subjected to internal pressure, R/h = 10.

Outer Crack, R/h = 10, ν = 0.3

a/h	c/a	L_o = 0.2h		L_o = 0.4h		L_o = 0.6h		L_o = 0.8h	
		$k_t(0)$	$k_b(0)$	$k_t(0)$	$k_b(0)$	$k_t(0)$	$k_b(0)$	$k_t(0)$	$k_b(0)$
1	1	.217	-.132	.130	-.0677	.0624	-.0182	.0189	.0027
	1.1	.233	-.116	.141	-.0605	.0676	-.0168	.0205	.0021
	1.5	.304	-.0535	.187	-.0299	.0907	-.0093	.0274	.0005
	2	.400	.0052	.248	.0016	.121	-.0001	.0366	-.0004
	10	.885	-.0013	.559	-.0006	.276	-.0002	.0829	.000
2	1	.431	.0057	.300	.0006	.161	-.0012	.0515	-.0008
	1.1	.470	.0234	.330	.0117	.178	.0030	.0571	-.0006
	1.5	.628	.0721	.448	.0447	.247	.0174	.0800	.0011
	2	.784	.0873	.566	.0574	.316	.0244	.103	.0026
	10	.938	.0002	.687	.0001	.389	.000	.127	.000
3	1	.648	.0738	.489	.0472	.287	.0195	.0982	.0019
	1.1	.699	.0822	.531	.0541	.315	.0234	.109	.0027
	1.5	.866	.0853	.670	.0607	.408	.0298	.144	.0053
	2	.972	.0547	.760	.0412	.468	.0220	.167	.0047
	10	.969	.000	.765	.000	.290	.000	.170	.000
10	1	1.030	-.0003	.921	.0016	.705	.0038	.337	.0029
	1.1	1.030	-.0032	.916	-.0012	.704	.0012	.339	.0016
	1.5	1.010	-.0013	.908	-.0012	.703	-.0008	.340	-.0002
	2	1.010	.0002	.911	.000	.706	.000	.343	.000
	10	1.020	.000	.917	.000	.716	.000	.350	.000

Inner Crack, R/h = 10, ν = 0.3

1	1	.215	.131	.127	.0659	.0607	.0171	.0187	-.0029
	1.1	.230	.114	.137	.0587	.0655	.0158	.0201	-.0023
	1.5	.301	.0529	.181	.0287	.0872	.0085	.0268	-.0006
	2	.395	-.0052	.239	-.0015	.116	.0001	.0355	.0004
	10	.872	.0012	.536	.0006	.261	.0002	.0796	.000
2	1	.424	-.0054	.286	.000	.149	.0018	.0482	.0011
	1.1	.463	-.0229	.313	-.0106	.164	-.0021	.0531	.0009
	1.5	.616	-.0707	.421	-.0415	.223	-.0145	.0727	-.0002
	2	.768	-.0855	.530	-.0529	.283	-.0202	.0925	-.0011
	10	.920	-.0002	.644	.000	.348	.000	.113	.000
3	1	.635	-.0721	.457	-.0430	.255	-.0154	.0863	-.0003
	1.1	.685	-.0804	.495	-.0494	.277	-.0187	.0944	-.0010
	1.5	.848	-.0834	.622	-.0553	.353	-.0238	.121	-.0028
	2	.952	-.0535	.705	-.0375	.405	-.0175	.140	-.0027
	10	.950	.000	.713	.000	.414	.000	.143	.000
10	1	1.020	.0005	.876	-.0023	.616	-.0038	.260	-.0022
	1.1	1.010	.0029	.874	.0003	.619	-.0018	.263	-.0015
	1.5	1.000	.0013	.871	.0010	.624	.0005	.269	.000
	2	1.010	-.0001	.875	.000	.631	.000	.273	.000
	10	1.100	.000	.882	.000	.642	.000	.281	.000

Table 5. Normalized stress intensity factors in a cylindrical shell with a fixed end containing an axial semielliptic surface crack and subjected to internal pressure, R/h = 25.

Outer Crack, R/h = 25, ν = 0.3

a/h	c/a	L_o = 0.2h		L_o = 0.4h		L_o = 0.6h		L_o = 0.8h	
		$k_t(0)$	$k_b(0)$	$k_t(0)$	$k_b(0)$	$k_t(0)$	$k_b(0)$	$k_t(0)$	$k_b(0)$
1	1	.161	-.201	.0957	-.102	.0456	-.0265	.0138	.0045
	1.1	.168	-.189	.101	-.0972	.0482	-.0260	.0146	.0040
	1.5	.204	-.140	.124	-.0747	.0598	-.0214	.0180	.0023
	2	.255	-.0860	.157	-.0469	.0759	-.0140	.0228	.0012
	10	.853	.0403	.534	.0225	.261	.0069	.0776	-.0005
2	1	.274	-.0909	.188	-.0574	.0991	-.0219	.0312	-.0012
	1.1	.297	-.0721	.205	-.0466	.109	-.0185	.0342	-.0013
	1.5	.397	-.0053	.280	-.0054	.150	-.0031	.0473	-.0007
	2	.524	.0488	.372	.0306	.202	.0119	.0637	.0006
	10	.908	-.0032	.656	-.0022	.362	-.0009	.114	.000
3	1	.411	-.0045	.306	-.0057	.174	-.0039	.0568	-.0011
	1.1	.449	.0140	.336	.0069	.193	.0015	.0631	-.0005
	1.5	.601	.0669	.458	.0454	.268	.0202	.0887	.0024
	2	.757	.0879	.582	.0628	.345	.0303	.116	.0047
	10	.936	.0002	.729	.0001	.439	.000	.148	.000
10	1	1.000	.0474	.894	.0420	.675	.0299	.306	.0108
	1.1	1.020	.0345	.908	.0317	.691	.0239	.317	.0094
	1.5	1.010	.0016	.915	.0031	.708	.0043	.332	.0028
	2	.991	-.0035	.898	-.0028	.698	-.0017	.329	-.0004
	10	.990	.000	.899	.000	.701	.000	.332	.000

Inner Crack, R/h = 25, ν = 0.3

1	1	.160	.200	.0948	.101	.0451	.0257	.0138	-.0047
	1.1	.168	.189	.0998	.0960	.0476	.0252	.0145	-.0041
	1.5	.203	.140	.122	.0734	.0588	.0206	.0178	-.0025
	2	.253	.0855	.154	.0459	.0743	.0133	.0225	-.0014
	10	.847	-.0400	.523	-.0218	.253	-.0065		
2	1	.272	.0904	.185	.0563	.0960	.0211	.0304	.0010
	1.1	.294	.0716	.201	.0456	.105	.0176	.0332	.0011
	1.5	.394	.0053	.272	.0052	.143	.0030	.0453	.0007
	2	.518	-.0483	.360	-.0293	.191	-.0107	.0603	-.0003
	10	.898	.0032	.632	.0021	.339	.0008	.107	.000
3	1	.407	.0046	.296	.0060	.164	.0042	.0534	.0013
	1.1	.444	-.0137	.324	-.0062	.180	-.0009	.0589	-.0008
	1.5	.594	-.0661	.438	-.0431	.247	-.0177	.0810	-.0015
	2	.747	-.0867	.555	-.0593	.316	-.0263	.104	-.0031
	10	.925	-.0002	.696	-.0001	.401	.000	.133	.000
10	1	.991	-.0467	.849	-.0392	.592	-.0245	.239	-.0069
	1.1	1.000	-.0341	.864	-.0296	.606	-.0199	.248	-.0062
	1.5	1.000	-.0017	.874	-.0032	.625	-.0040	.261	-.0021
	2	.982	.0034	.860	.0026	.620	.0013	.261	.0002
	10	.981	.000	.862	.000	.626	.000	.266	.000

Table 6. Normalized stress intensity factors in a cylindrical shell with a fixed end containing an axial semielliptic surface crack and subjected to internal pressure, R/h = 100.

Outer Crack, R/h = 100, ν = 0.3

a/h	c/a	L_o = 0.2h		L_o = 0.4h		L_o = 0.6h		L_o = 0.8h	
		$k_t(0)$	$k_b(0)$	$k_t(0)$	$k_b(0)$	$k_t(0)$	$k_b(0)$	$k_t(0)$	$k_b(0)$
1	1	.130	-.273	.0768	-.138	.0365	-.0355	.0111	.0063
	1.1	.132	-.267	.0788	-.136	.0376	-.0360	.0114	.0058
	1.5	.144	-.239	.0871	-.126	.0419	-.0353	.0126	.0044
	2	.160	-.204	.0982	-.109	.0474	-.0316	.0142	.0034
	10	.582	.0702	.362	.0386	.176	.0116	.0521	-.0010
2	1	.172	-.217	.117	-.134	.0610	-.0493	.0191	-.0016
	1.1	.180	-.204	.123	-.127	.0646	-.0479	.0202	-.0020
	1.5	.217	-.151	.152	-.0972	.0804	-.0385	.0251	-.0023
	2	.271	-.0921	.191	-.0607	.102	-.0248	.0318	-.0018
	10	.906	.0431	.647	.0288	.351	.0121	.109	.0010
3	1	.224	-.153	.165	-.105	.0923	-.0458	.0296	-.0049
	1.1	.240	-.136	.178	-.0944	.0999	-.0420	.0321	-.0048
	1.5	.310	-.0689	.234	-.0501	.133	-.0238	.0429	-.0033
	2	.406	-.0047	.308	-.0046	.178	-.0029	.0573	-.0007
	10	.943	.0009	.725	.0007	.424	.0004	.138	.000
10	1	.689	.0828	.609	.0678	.441	.0414	.178	.0108
	1.1	.740	.0891	.655	.0739	.479	.0464	.196	.0128
	1.5	.901	.0835	.805	.0722	.599	.0493	.254	.0160
	2	.992	.0477	.891	.0426	.670	.0308	.288	.0111
	10	.975	.000	.880	.000	.667	.000	.289	.000

Inner Crack, R/h = 100, ν = 0.3

1	1	.130	.273	.0767	.137	.0365	.0353	.0111	-.0064
	1.1	.132	.267	.0787	.136	.0375	.0359	.0114	-.0058
	1.5	.144	.239	.0869	.126	.0418	.0350	.0126	-.0044
	2	.160	.204	.0979	.109	.0472	.0313	.0142	-.0035
	10	.581	-.0700	.359	-.0382	.174	-.0113	.0517	.0011
2	1	.172	.217	.116	.133	.0605	.0486	.0190	.0014
	1.1	.179	.204	.123	.126	.0640	.0471	.0201	.0018
	1.5	.217	.150	.150	.0963	.0793	.0376	.0248	.0021
	2	.271	.0918	.189	.0599	.100	.0241	.0313	.0016
	10	.902	-.0429	.638	-.0283	.342	-.0115	.106	-.0008
3	1	.224	.153	.164	.104	.0908	.0448	.0291	.0046
	1.1	.239	.136	.176	.0934	.0981	.0410	.0315	.0045
	1.5	.309	.0687	.230	.0493	.130	.0229	.0417	.0030
	2	.404	.0047	.303	.0045	.172	.0028	.0553	.0006
	10	.938	-.0009	.711	-.0007	.408	-.0004	.132	.000
10	1	.684	-.0821	.591	-.0691	.409	-.0370	.156	-.0081
	1.1	.734	-.0884	.635	-.0711	.442	-.0416	.170	-.0098
	1.5	.894	-.0829	.779	-.0695	.549	-.0440	.216	-.0121
	2	.985	-.0473	.863	-.0410	.614	-.0275	.244	-.0084
	10	.969	.000	.854	.000	.614	.000	.247	.000

Table 7. Normalized stress intensity factors in a cylindrical shell with a fixed end containing an axial semielliptic surface crack and subjected to internal pressure, R/h = 200.

Outer Crack, R/h = 200, ν = 0.3

a/h	c/a	L_o = 0.2h		L_o = 0.4h		L_o = 0.6h		L_o = 0.8h	
		$k_t(0)$	$k_b(0)$	$k_t(0)$	$k_b(0)$	$k_t(0)$	$k_b(0)$	$k_t(0)$	$k_b(0)$
1	1	.124	-.297	.0734	-.150	.0349	-.0385	.0106	.0069
	1.1	.126	-.293	.0749	-.149	.0357	-.0395	.0108	.0064
	1.5	.133	-.273	.0802	-.144	.0385	-.0401	.0116	-.0227
	2	.142	-.247	.0867	-.132	.0418	-.0380	.0126	.0041
	10	.426	.0261	.264	.0143	.128	.0043	.0380	-.0004
2	1	.152	-.263	.103	-.162	.0535	-.0595	.0168	-.0018
	1.1	.156	-.253	.107	-.158	.0558	-.0591	.0175	-.0023
	1.5	.177	-.212	.124	-.136	.0654	-.0533	.0204	-.0031
	2	.209	-.162	.147	-.106	.0783	-.0426	.0243	-.0028
	10	.797	.0801	.568	.0532	.306	.0221	.0948	.0017
3	1	.183	-.216	.134	-.148	.0747	-.0637	.0239	-.0065
	1.1	.192	-.202	.142	-.139	.0794	-.0614	.0254	-.0067
	1.5	.234	-.144	.176	-.103	.0998	-.0474	.0320	-.0060
	2	.295	-.0821	.223	-.0596	.128	-.0284	.0410	-.0039
	10	.942	.0364	.721	.0266	.420	.0129	.135	.0019
10	1	.504	-.0314	.444	.0242	.318	.0131	.124	.0026
	1.1	.549	.0482	.485	.0387	.349	.0227	.137	.0054
	1.5	.719	.0876	.639	.0744	.468	.0486	.190	.0142
	2	.873	.0880	.780	.0767	.577	.0525	.238	.0168
	10	.972	.000	.874	.000	.652	.000	.273	.000

Inner Crack, R/h = 200, ν = 0.3

1	1	.124	.297	.0734	.149	.0349	.0384	.0106	-.0069
	1.1	.126	.293	.0748	.149	.0357	.0394	.0108	-.0064
	1.5	.132	.273	.0801	.143	.0385	.0400	.0116	.0051
	2	.142	.247	.0866	.132	.0417	.0378	.0126	-.0042
	10	.425	-.0261	.263	-.0142	.127	-.0042	.0378	.0004
2	1	.151	.263	.103	.162	.0533	.0591	.0167	.0017
	1.1	.156	.253	.107	.157	.0556	.0587	.0174	.0022
	1.5	.177	.211	.123	.135	.0650	.0527	.0203	.0029
	2	.209	.162	.146	.105	.0777	.0420	.0242	.0027
	10	.795	-.0799	.563	-.0527	.302	-.0215	.0934	-.0015
3	1	.183	.216	.134	.147	.0741	.0629	.0237	.0063
	1.1	.191	.202	.141	.139	.0786	.0605	.0252	.0065
	1.5	.233	.144	.174	.102	.0985	.0465	.0315	.0057
	2	.294	.0819	.221	.0589	.126	.0276	.0403	.0036
	10	.939	-.0363	.713	-.0262	.410	-.0124	.132	-.0017
10	1	.502	.0312	.436	-.0233	.303	-.0118	.114	-.0018
	1.1	.546	-.0479	.475	-.0376	.332	-.0210	.126	-.0043
	1.5	.715	-.0871	.625	-.0725	.441	-.0451	.170	-.0118
	2	.868	-.0876	.762	-.0746	.542	-.0484	.212	-.0137
	10	.967	.000	.855	.000	.614	.000	.243	.000

Table 8. Distribution of the normalized stress intensity factors along the crack front in a cylindrical shell containing an axial semi-elliptic surface crack and subjected to internal pressure, $\bar{x} = (x_1+c)/a$, R/h = 10, a/h = 1, c/a = 1.1.

L_o/h	0.2		0.4		0.6		0.8	
	k_t	k_b	k_t	k_b	k_t	k_b	k_t	k_b
$\bar{x}$	Outer Crack, R/h = 10, a/h = 1, c/a = 1.1							
.929	.0882	-.247	.0615	-.170	.0310	-.0799	.0095	-.0212
.828	.106	-.247	.0685	-.145	.0339	-.0590	.0106	-.0128
.688	.127	-.231	.0806	-.122	.0394	-.0442	.0128	-.0055
.516	.153	-.203	.0958	-.102	.0467	-.0318	.0148	-.0005
.319	.183	-.169	.113	-.0837	.0556	-.0229	.0168	.0019
.108	.216	-.133	.131	-.0676	.0635	-.0181	.0193	.0026
0	.233	-.116	.141	-.0605	.0676	-.0168	.0205	.0021
-.108	.248	-.0990	.149	-.0539	.0716	-.0161	.0216	.0012
-.319	.275	-.0687	.164	-.0420	.0785	-.0153	.0236	-.0010
-.516	.293	-.0433	.175	-.0316	.0829	-.0144	.0257	-.0026
-.688	.298	-.0231	.179	-.0224	.0846	-.0126	.0267	-.0034
-.828	.288	-.0085	.176	-.0147	.0840	-.0103	.0259	-.0034
-.929	.258	.0004	.167	-.0089	.0818	-.0082	.0251	-.0031
	Inner Crack, R/h = 10, a/h = 1, c/a = 1.1							
.929	.0886	.247	.0619	.169	.0310	.0794	.0094	.0210
.828	.106	.246	.0683	.144	.0334	.0582	.0104	.0125
.688	.127	.230	.0796	.121	.0386	.0431	.0124	.0052
.516	.152	.202	.0941	.100	.0454	.0306	.0144	.0003
.319	.182	.167	.110	.0818	.0533	.0217	.0164	-.0022
.108	.214	.132	.128	.0658	.0615	.0170	.0189	-.0028
0	.230	.114	.137	.0587	.0655	.0158	.0201	-.0023
-.108	.246	.0980	.145	.0522	.0694	.0151	.0212	-.0013
-.319	.273	.0680	.160	.0407	.0761	.0144	.0231	.0008
-.516	.291	.0428	.171	.0306	.0805	.0136	.0251	.0024
-.688	.297	.0229	.175	.0217	.0821	.0119	.0260	.0032
-.828	.286	.0084	.173	.0142	.0817	.0097	.0251	.0032
-.929	.257	.0004	.165	.0085	.0796	.0077	.0242	.0029

Table 9. Distribution of the normalized stress intensity factors along the crack front in a cylindrical shell containing an axial semi-elliptic surface crack and subjected to internal pressure, $\bar{x} = (x_1+c)/a$, R/h = 10, a/h = 1.

L_o/h	0.2		0.4		0.6		0.8	
	k_t	k_b	k_t	k_b	k_t	k_b	k_t	k_b
$\bar{x}$	Outer Crack, R/h = 10, a/h = 1, c/a = 2							
.929	.161	-.0858	.124	-.0555	.0688	-.0252	.0226	-.0067
.828	.202	-.0813	.143	-.0456	.0755	-.0180	.0246	-.0038
.688	.245	-.0668	.165	-.0338	.0845	-.0116	.0277	-.0012
.516	.291	-.0469	.190	-.0222	.0951	-.0062	.0302	.0002
.319	.337	-.0252	.214	-.0117	.106	-.0028	.0324	.0005
.108	.381	-.0044	.238	-.0025	.117	-.0008	.0352	.000
0	.400	.0052	.248	.0016	.121	-.0001	.0366	-.0004
-.108	.418	.0141	.258	.0055	.126	.0006	.0378	-.0007
-.319	.443	.0292	.272	.0126	.132	.0025	.0399	-.0008
-.516	.454	.0404	.278	.0190	.135	.0052	.0421	-.0003
-.688	.446	.0476	.277	.0247	.134	.0085	.0429	.0009
-.828	.419	.0503	.266	.0294	.131	.0119	.0411	.0026
-.929	.369	.0480	.249	.0327	.126	.0153	.0396	.0041
	Outer Crack, R/h = 10, a/h = 1, c/a = 10							
.929	.592	.0022	.429	.0013	.230	.0005	.0742	.0001
.828	.693	.0020	.468	.0010	.241	.0003	.0774	.000
.688	.770	.0013	.503	.0006	.253	.0001	.0821	.000
.516	.827	.0006	.531	.0002	.265	.000	.0832	.000
.319	.865	-.0002	.549	-.0002	.273	-.0001	.0825	.000
.108	.883	-.0009	.558	-.0005	.276	-.0002	.0828	.000
0	.885	-.0013	.559	-.0006	.276	-.0002	.0829	.000
-.108	.881	-.0016	.558	-.0008	.276	-.0002	.0827	.000
-.319	.860	-.0020	.547	-.0010	.272	-.0003	.0822	.000
-.516	.820	-.0024	.527	-.0013	.263	-.0004	.0827	.000
-.688	.762	-.0026	.498	-.0015	.251	-.0006	.0815	.000
-.828	.684	-.0024	.463	-.0016	.239	-.0007	.0768	-.0002
-.929	.583	-.0013	.424	-.0017	.227	-.0009	.0736	-.0002

Table 10. Distribution of the normalized stress intensity factors along the crack front in a cylindrical shell containing an axial semi-elliptic surface crack and subjected to internal pressure, $\bar{x} = (x_1+c)/a$, R/h = 10, c/a = 1.1.

L_o/h	0.2		0.4		0.6		0.8	
	k_t	k_b	k_t	k_b	k_t	k_b	k_t	k_b
$\bar{x}$	Inner Crack, R/h = 10, a/h = 3, c/a = 1.1							
.929	.104	.174	.0842	.123	.0571	.0633	.0236	.0191
.828	.159	.143	.126	.0912	.0811	.0414	.0317	.0106
.688	.244	.0829	.191	.0476	.117	.0187	.0439	.0031
.516	.362	.0169	.275	.0069	.162	.0007	.0581	-.0006
.319	.498	-.0373	.369	-.0242	.212	-.0104	.0729	-.0014
.108	.629	-.0711	.458	-.0436	.258	-.0166	.0879	-.0010
0	.685	-.0804	.495	-.0494	.277	-.0187	.0944	-.0010
-.108	.731	-.0850	.526	-.0529	.293	-.0205	.0993	-.0014
-.319	.787	-.0840	.563	-.0547	.313	-.0233	.106	-.0033
-.516	.794	-.0745	.566	-.0517	.316	-.0250	.109	-.0053
-.688	.755	-.0619	.538	-.0466	.302	-.0254	.107	-.0070
-.828	.676	-.0488	.483	-.0401	.277	-.0241	.0989	-.0080
-.929	.559	-.0364	.409	-.0326	.243	-.0217	.0894	-.0081
	Inner Crack, R/h = 10, a/h = 10, c/a = 1.1							
.929	.226	.0164	.176	.0091	.123	.0023	.0598	-.0005
.828	.431	-.0519	.334	-.0411	.226	-.0254	.103	-.0094
.688	.688	-.0791	.544	-.0584	.366	-.0332	.160	-.0105
.516	.894	-.0547	.726	-.0410	.494	-.0235	.212	-.0071
.319	.996	-.0187	.835	-.0163	.579	-.0110	.244	-.0039
.108	1.020	.000	.874	-.0024	.616	-.0037	.260	-.0021
0	1.010	.0029	.874	.0003	.619	-.0018	.263	-.0015
-.108	1.010	.0033	.867	.0012	.615	-.0008	.261	-.0010
-.319	.965	.0018	.822	.0011	.581	.000	.249	-.0005
-.516	.898	.0006	.744	.0005	.518	.000	.227	-.0003
-.688	.805	-.0003	.643	-.0006	.438	-.0006	.195	-.0004
-.828	.688	.0001	.526	.0005	.350	.0004	.157	.000
-.929	.549	.0001	.407	.0004	.266	.0004	.120	.000

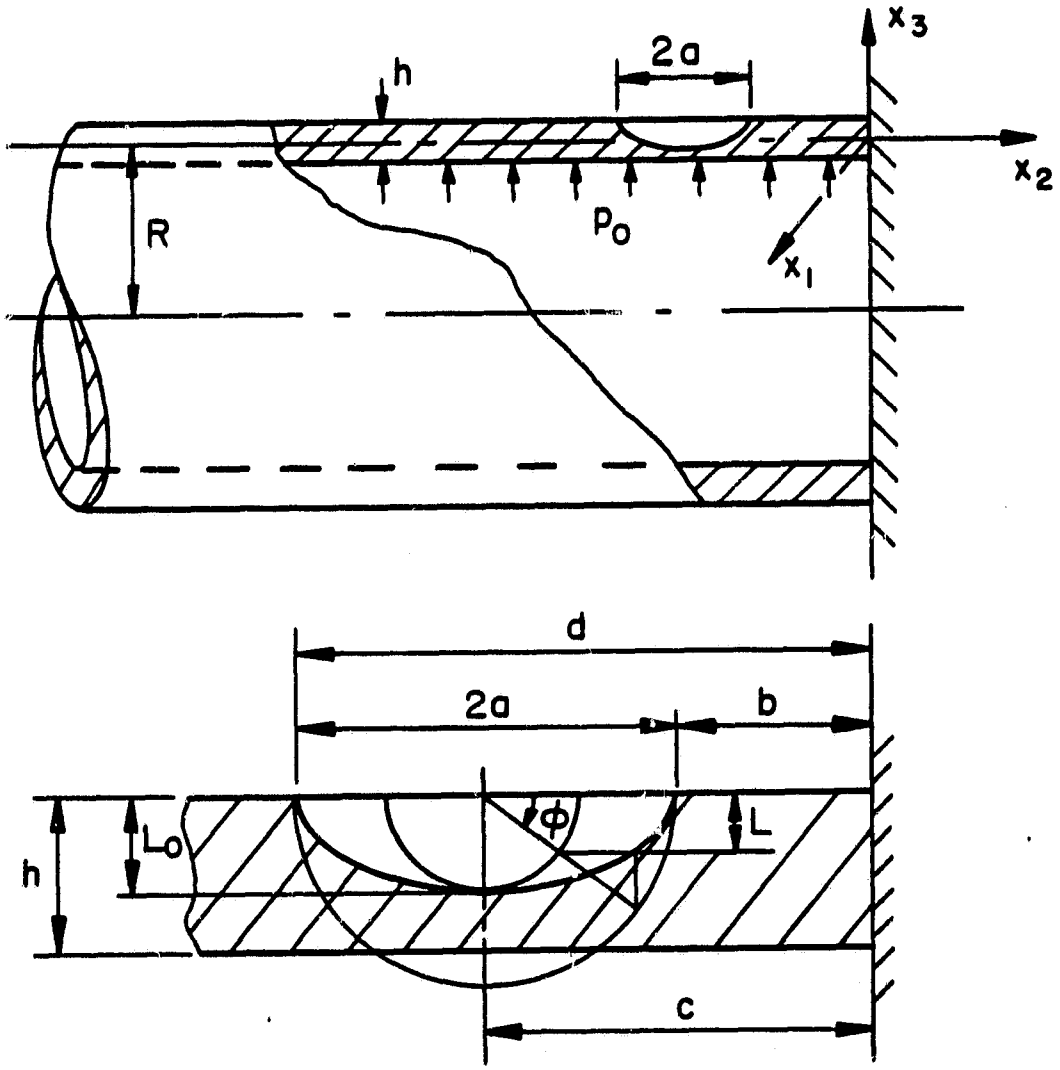

Fig. 1 Geometry and notation for a cylindrical shell with a fixed end which contains a part-through ($L<h$) or a through ($L(x_2)=h$, $-d<x_2<-b$) crack.

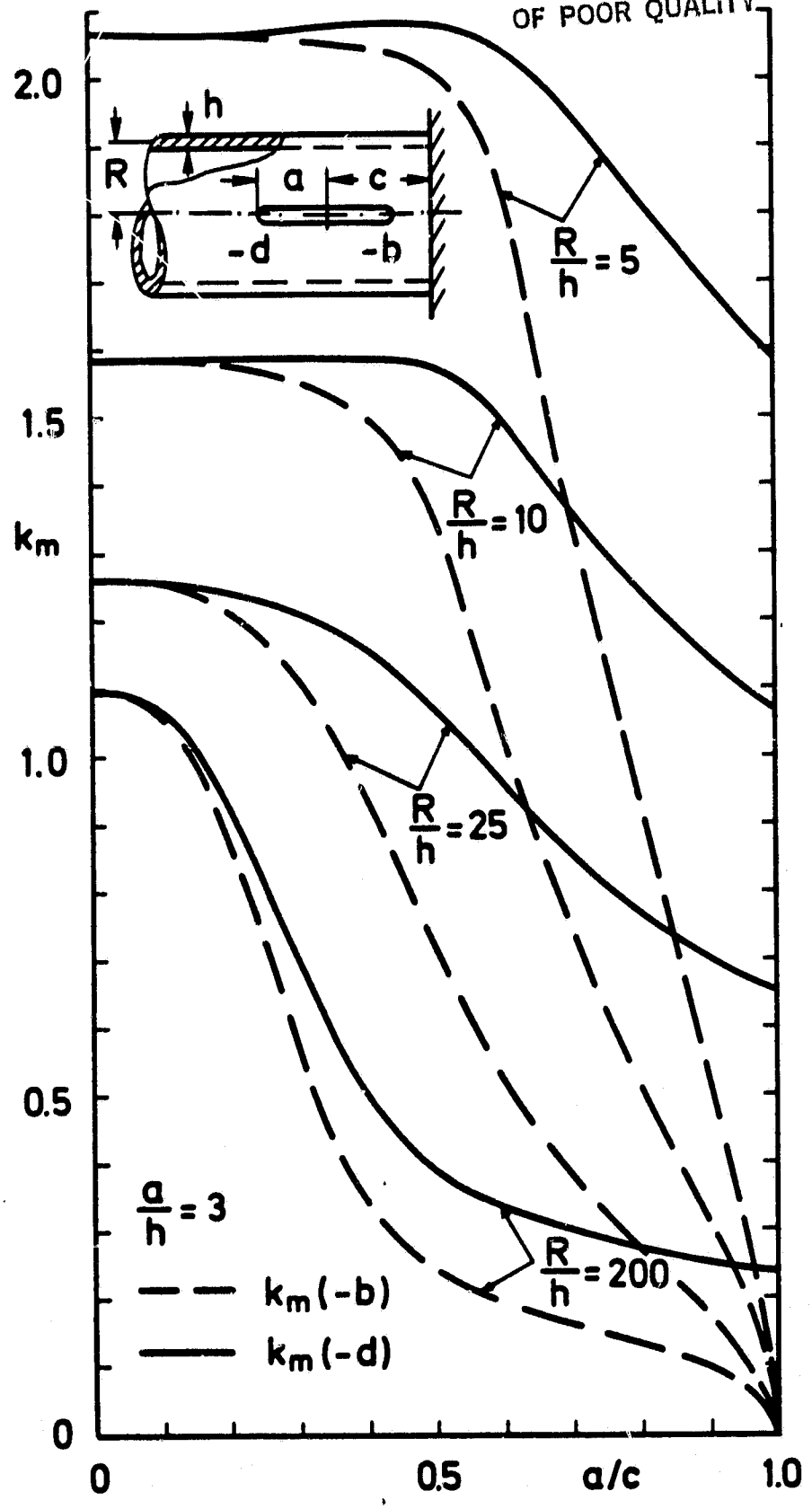

Fig. 2 Membrane component of the normalized stress intensity factor at the end points of an axial through crack in a pressurized cylinder with a fixed end, $\nu=0.3$, $a/h = 3$.

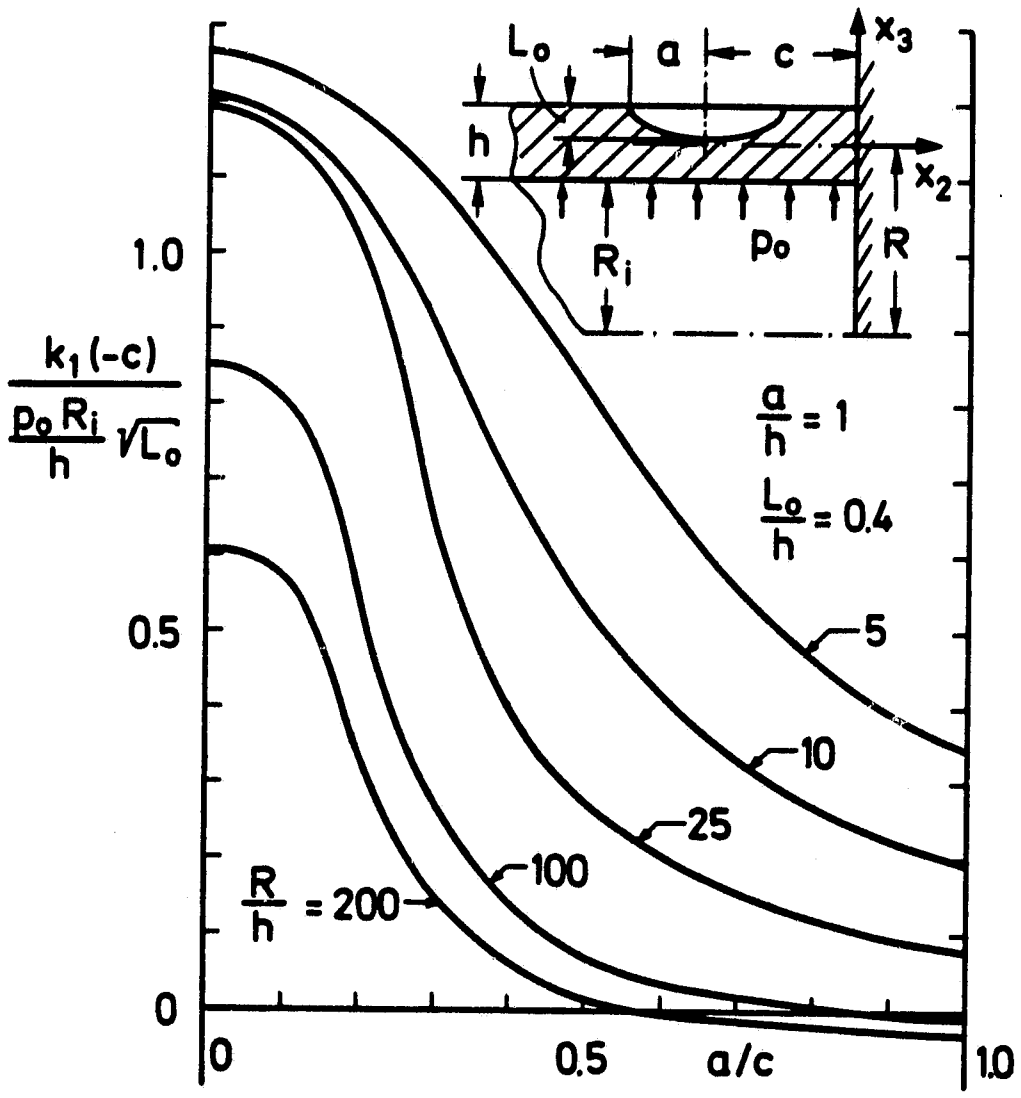

Fig. 3 Normalized total stress intensity factor at the maximum penetration point ($L=L_o$, $x_2=-c$) of a semi-elliptic outer crack in a pressurized cylinder with a fixed end, $\nu = 0.3$, $L_o/h = 0.4$, $a/h = 1$.

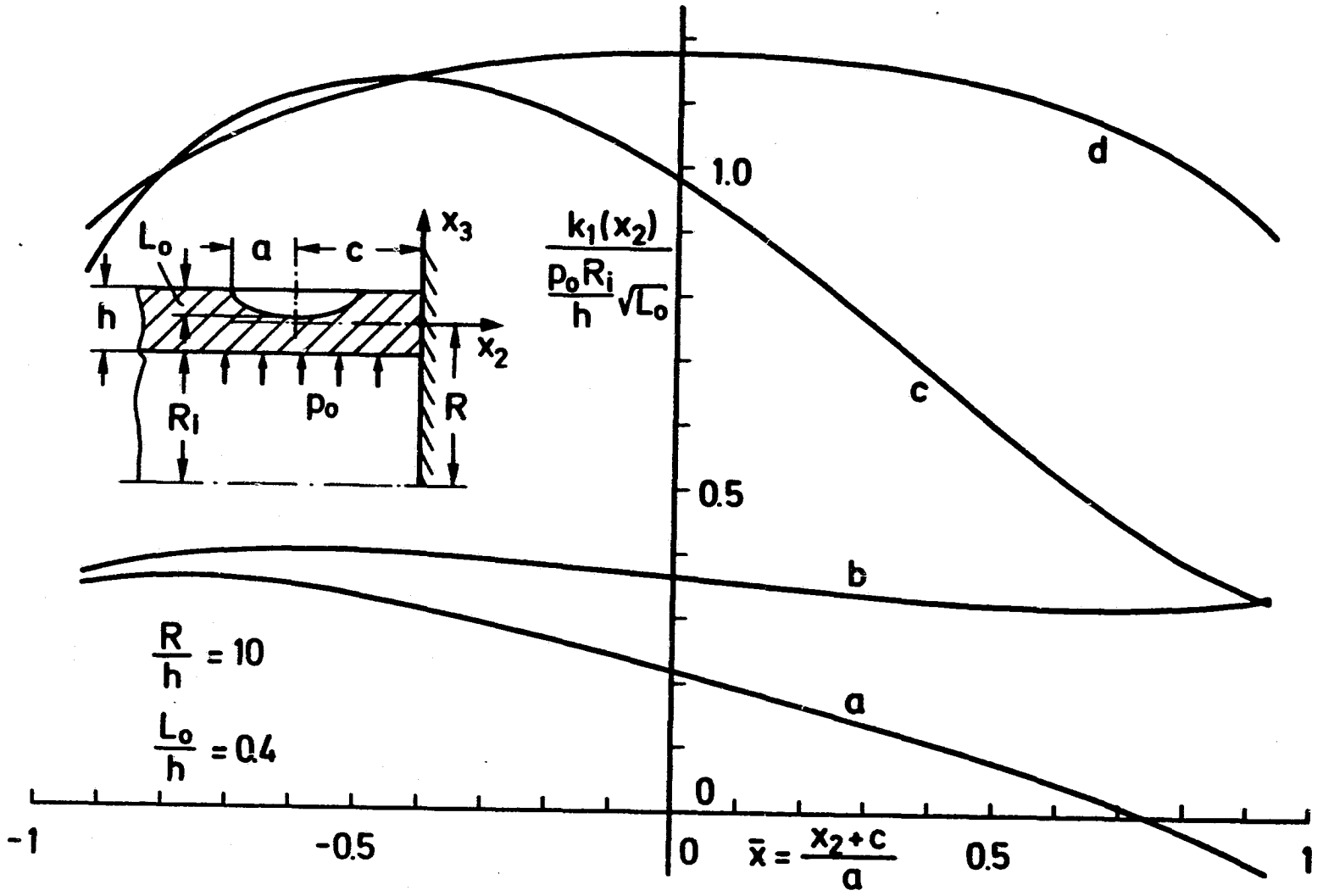

Fig. 4 Distribution of the normalized total stress intensity factor along the border of a part-through semi-elliptic surface crack in a pressurized cylinder with a fixed end, $\nu = 0.3$, $L_o/h = 0.4$, $R/h = 10$. Curve a: outer crack, $a/h = 1$, $c/a = 1.1$; curve b: inner crack, $a/h = 1$, $c/a = 1.1$; curve c: inner crack, $a/h = 3$, $c/a = 1.1$; curve d: outer crack, $a/h = 1$, $c/a = 10$.